UNIVERSITY OF MISKOLC

OPTIMIZATION OF PARAFFIN REMOVAL FROM THE ALGYO – SZAZHALOMBATTA TRANSPORTING CRUDE OIL PIPELINE

PhD Thesis

by

Farag Mohamed ABDUMULA

A dissertation presented to the Doctoral School of Earth Sciences
of the University of Miskolc in partial fulfillment of the requirements for the degree
of
Doctor of Philosophy in the discipline of Petroleum Engineering

Miskolc - 2005

ABSTRACT

Pipelines are the most important petroleum supply line, including crude oil, refined fuel and raw materials. Because of the volume that must be transported, pipelines are the only feasible method for moving the enormous quantities of petroleum and its products.

In addition to their efficiency, pipelines also have important environmental and safety benefits. Compared to other inland transport modes, pipelines do not crowd our highways and rivers and they produce negligible air pollution. Pipelines also have a lower spill rate per barrel of oil transported than competing modes of transportation, namely trucks and barges.

In colder environs, oil carrying pipelines lose heat rapidly. This is especially true for over ground pipelines in colder regions of the world. If the temperature of the oil falls below the "Wax Appearance Point' (WAP), wax will generally deposit on the walls of the pipeline. This deposited wax increases in thickness due to continued deposition and also ages due to an increase in its wax content. The former may lead to plugging of the complete pipe cross-section, while the latter leads to hardening of the deposited wax. Decreased pipe diameters are a major concern to oil transportation companies as they represent a major increase in pumping costs, not to mention the loss of throughput and quality of oil.

In the aforementioned extreme cases of deposition, routine shutdown has to be scheduled to pig the pipeline. Hence, establishing mechanisms of wax deposition

would help in identifying the parameters that would need to be controlled in order to check wax deposition.

The crude oil produced at Algyo field is transported through the Algyo-Szazhalombatta pipeline to the refinery. To improve the transporting conditions, the crude is mixed with gasoline. The high paraffin contents of the crude cause heavy paraffin deposition on the pipe wall. This paraffin precipitation increases the transporting costs and finally can totally stop the transportation. In this project, deposition of wax on the wall of oil pipelines is regarded as a problem since the tube diameter is reduced. Consequently, more power is needed to force the same amount of oil through the system. A mathematical model for quantitative prediction of wax deposition has been developed. The project requires both experimental measurements and theoretical model development. The models developed can be used as a basis for designing prevention and remediation techniques. The influence of paraffin thickness on selected pipe section is also shown. Finally an economical study of economic interval for the pigging process is a presented.

ACKNOWLEDGMENTS

First of all, I praise to Allah Subhanahu wa Ta`aalaa that I concluded this work.

It is a great pleasure to acknowledge with sincere thanks and deep appreciation tothe General People's Committee of Education for giving me the opportunity to pursue a higher qualification

For the success of my project, I would like to acknowledge Prof. Gabor Takacs who has helped in making this work a success, for his guidance and advice. I am also much indebted to Mr.: Zoltan Turzo. This thesis would not be as special without their efforts. Without their expertise this work would not have been possible.

Though my parents may not have taught me how to generate a study, their eternal support, love and confidence in their son contributed significantly in making me the individual I am today.

This is a big "thank you" to my wife for her support, encouragement and for her perseverance.

Finally, I would like to express my appreciation to every person who contributed with either inspirational or actual work to this thesis

Dedication

I wish to dedicate this work to the spirit of my father, my greatest Mum, my wife and brothers who were the main source of support since their images in my heart and their words provoked my diligence.

They contributed to this effort in ways that I probably will never know or understand. Without whom my study would have been impossible.

Farag

Table of Contents

INTRODUCTION 10

1. **Literature Review** 12

1.1 Rheological Properties of waxy Crude Oils 12
1.2 Paraffin Deposition in Crude Oil Transporting Pipelines 20

2. **History of the Algyo-Kiskunhalas-Szazhalombatta pipeline** 28

3. **Rheological Properties of Algyo and Kiskunhalas Crude Oils** 33

3.1 Introduction 33
3.2 Properties of Non-Newtonian Fluids 34
3.3 General Equations for Non-Newtonian Fluids 36
3.3.1 The Method of Dodge and Metzner 37
3.3.2 Derivation of the BNS equation 38
3.4 Determination of Flow Curves 46
3.4.1 Introduction 46
3.4.2 Measurements with Extrusion Viscometer 46
3.4.3 Measurements with Rotary Viscometers 46
3.4.4 Haake Rot23 (100/300) Sensor System 49
3.4.5 Description 49
3.5 Experimental Procedures 50
3.5.1 Thixotropic Checking 51
3.5.2 Flow Curves 53
3.5.3 The Laboratory Experiment 53
3.6 Measurement Results 54
3.6.1 Algyo Crude Oil Sample 54
3.6.2 Kiskunhalas Crude Oil Sample 54
3.7 Density Measurement 58

4. **Development of a Procedure to describe the Growth** 60

of Paraffin Deposition in Pipelines 60

4.1 Introduction 60
4.2 Background Theories 60
4.3 Calculations of Non-Isothermal Pressure Drop in the Pipelines. 62
4.3.1 Non-Isothermal Oil Transport 62
4.3.2 Temperature distribution along the pipeline 63
4.3.3 Frictional pressure drop calculations 67
4.4 Description of the Growth of Paraffin Deposition in Pipelines 68
4.4.1 Introduction 68

4.4.2 Determination of Friction Factor and Pipe Roughness for a Clean Pipe 69
4.4.3 Development of the Mathematical Model to Describe the Influence of the Paraffin Deposition on the Pipe ID 71
4.4.4 Calculating the Pipe ID-Time Function 75

5. **Economic conditions of pigging operations** 77

5.1 Introduction 77
5.2 Pressure Drop Due to Paraffin Accumulation 77
5.3 Additional Pumping Cost 79
5.4 Calculation of the most Economic Pigging interval 80

6. **Calculation results** 82

6.1 Introduction 82
6.2 Paraffins in the Algyo oil field 82
6.3 Paraffin deposition in the Algyo –Szazhalombatta pipeline 84
6.3.1 Field Data 84
6.3.2 Use of Field Data 86
6.4 Calculation Procedure 87
6.4.1 Temperature distribution along the pipeline 90
6.4.2 Determination of the pipe roughness from data taken from the clean pipe 92
6.4.3 Determination of the Waxy ID of the Pipeline 93
6.5 Determination of additional pressure loss vs. time equation 98
6.6 Additional Pumping Cost due to Additional Pressure Drop 101
6.7 Calculation of the most Economic Pigging interval 102

7. **Conclusions** 104

8. **List of references** 106

List of Figures

Fig. 1-1 Algyo-Szazhalombatta pipeline profile. 30
Fig. 1-2 Kiskunhalas-Palmonostora pipeline profile. 31
Fig. 3-1 Shear thinning fluid. 34
Fig. 3-2 Flow curves of different types of fluid. 34
Fig. 3-3 Components of a force balance. 36
Fig. 3-4 Friction factor for turbulent flow of a pseudoplastic fluid n=0.4 45
Fig. 3-5 Friction factor for turbulent flow of a pseudoplastic fluid n=0.6 45
Fig. 3-6 Rotary viscometer. 47
Fig. 3-7 Haake device. 50
Fig. 3-8 Thixotropic checking for Algyo crude oil at 5ºC. 52
Fig. 3-9 Thixotropic checking for Kiskunhalas crude oil. 52
Fig. 3-10 Measured flow curves for Algyo crude oil. 56
Fig. 3-11 Calculated flow curves for Algyo crude oil. 56
Fig. 3-12 Measured flow curves for Kiskunhalas crude oil. 57
Fig. 3-13 Calculated flow curves for Kiskunhalas crude oil. 57
Fig. 3-14.Algyo and Kiskunhalas crude oil densities 59
Fig. 4-1 Wax accumulation in crude oil pipeline. 61
Fig. 4-2 Heat transfer coefficient related to pipeline diameter. 65
Fig. 4-3 Influence of time on the pressure drop and pipe ID. 75
Fig. 5-1 Economic interval for pipeline pigging. 81
Fig. 6-1 Paraffin properties of Algyo crude oil samples at 20ºC 83
Fig. 6-2 Paraffin in Algyo field. 84
Fig. 6-3 Algyo-Szazhalombatta pipeline control system. 85
Fig. 6-4 Total energy curves before pigging. 88
Fig. 6-5 Total energy curves after pigging 89
Fig. 6-6 Total energy curves before and after pigging. 89
Fig. 6-7 Temperature distribution in Algyo-Szazhalombatta pipeline. 91
Fig. 6-8 Flow chart of the paraffin thickness calculation. 94
Fig. 6-9 Paraffin influence on pipe diameter. 97
Fig. 6-10 Deposition thicknesses. 98
Fig. 6-11 Additional pressure drop in Algyo-Szazhalombatta pipeline. 100
Fig. 6-12 Economic interval for Algyo-Szazhalombatta pipeline Pigging. 103

List of Tables

Table 1-1 Algyo-Szazhalombatta transporting pipeline 29
Table 1-2 Kiskunhalas-Szank-Palmonostora pipeline 29
Table 3-1 Algyo crude oil rheological properties. 55
Table 3-2 Kiskunhalas crude oil rheological properties 55
Table 3-3 Algyo and Kiskunhalas crude oil densities.....59
Table 6-1.Paraffin Properties of Algyo oil.....83
Table 6-2 Sample of data collected from the pipeline 86
Table 6-3 Data used for calculations. 87
Table 6-4 The energy curves data. 88
Table 6-5 Friction factor for pipeline sections. 90
Table 6-6. Temperatures and rheological indexes. 91
Table 6-7 Calculated pipeline roughness for all sections for clean pipe. 93
Table 6-8 Reynolds number for all sections.....93
Table 6-9. Sovenyhaza-Palmonostora section. 95
Table 6-10. Palmonostora-Kiskunfelegyhaza section.....96
Table 6-11. Kiskunfelegyhaza-Kecskemet section 96
Table 6-12. Average effected pipe diameter and paraffin thickness. 97
Table 6-13 Pressure at pipeline sections. 99
Table 6-14 Pressure drops between the sections 99
Table 6-15 The total pressure drop. 100
Table 6-16 The additional pump cost. 101
Table 6-17 The additional pumping cost and one pigging cost.....103

INTRODUCTION

Pipelines play an important role in the transportation of petroleum and its derivatives, since they affect daily lives in most parts of the world. Modern people's lives are based on an environment in which energy plays a predominant role. Oil and gas are the major participants in the supply of energy, and pipelines are the primary means by which they are transported. It is no coincidence that an extensive pipeline network goes hand-in-hand with a high standard of living and technological progress.

The main objective of this dissertation is to investigate the transporting conditions of the Algyo-Szazhalombatta crude oil transporting pipeline. The starting point in this work is a review of some significant works about the rheological properties of crude oils and wax deposition in crude oil transporting pipelines. A brief description of the Algyo-Szazhalombatta crude oil transporting pipeline operation's history is shown in the Second Chapter. An extensive study of the rheological characteristics of transported crude oil is indispensable for determining the behavior of crude oil, general classification of fluids and laboratory measurements are mentioned in the Third Chapter.

Paraffin formation and deposition on the wall of crude oil transporting pipelines is regarded as a problem in the oil transportation industry since it reduces the throughput. Therefore, more power is required to force the same amount of crude oil through the system. This deposited wax increases in thickness due to continued deposition and also ages due to an increase in its wax content. The former may lead to plugging of the complete pipe cross-section, while the latter leads to hardening of the

deposited wax. Decreased pipe diameters are a major concern to oil transportation companies as they represent a major increase in pumping cost and increased pipe wall friction. In the Fourth Chapter paraffin deposition in the Algyo-Szazhalombatta pipeline is discussed and the task is accomplished using the calculation model developed in this dissertation. To describe the time variation of the paraffin layer thickness, and consequently the pipeline's inside diameter, a calculation model is developed which is based on measured pressure drops vs time. The proposed calculations of the additional pressure drop due to paraffin deposition have been described as well.

One option with the Pipeline Company is to regularly scrape and clean the wax from the pipeline walls by what is called pigging. An economical study concerning the additional pumping costs caused by paraffin deposition of the Algyo-Szazhalombatta pipeline, which involves the pigging operation, is the focus point of Chapter Five. Applications on the derived model are presented in the Chapter Six. At the end of this work under the subtitle Conclusions the reader can enjoy a short summary of the author's main findings concerning the studied pipeline system.

CHAPTER 1
LITERATURE REVIEW

1.1 Rheological Properties of waxy Crude Oils

Lozano et al. [1] studied the resistivity and viscosity of asphaltic crude and waxy crudes for various shear rates and shearing time at different test temperatures and ages in a Fan Viscosimeter modified for this purpose. The relationship between resistivity and viscosity for both crudes and their fractions is correlated by an equation of the general form: mn R = k 10 where (R) is the resistivity, (n) is the viscosity, and (K) and (m) are constants to be determined experimentally. The application of voltage to waxy crude greatly reduces its viscosity and hard asphalt and polyethylene can efficiently inhibit paraffin deposition. The constituents of waxy crudes primarily responsible for the anomalous flow behavior are the waxes. The waxes are also responsible for the time dependency observed and for the deposits formed. The results suggest the presence of a micellar structure of which waxes are the main constituents in an oil base. From the contribution of waxes, asphaltenes and resins to the electrical resistivity of waxy and asphaltic crudes it can be concluded that the structures formed are of very different nature. Observations and viscosity-resistivity data support a proposed mechanism for the formation of paraffin deposits in pipes. The results show also that viscosity and resistivity curves represent simple diagnostic tools, which show the temperature range at which deposit micelles may form.

Matlach et al. [2] The Altamont area in Utah produces one of the highest wax content crudes anywhere in the world. These high pour point and hard to handle crude

oils are an even tougher problem because of their location in a geographical area subject to very low ambient temperatures. Millions of dollars are spent each year heating these crudes in order to expedite their production and transportation. Crude oil samples from the area have been tested using a variety of techniques. Paraffin deposition, viscosity, cloud point, pour point, yield values, wax extraction and GLC tests have been conducted in order to characterize the crude oil samples. The effects of various chemical additives were then analyzed using the same tests. The effective paraffin inhibitors not only reduced the quantity of wax deposited, but dramatic shifts in molecular weight range and configuration were also apparent. GLC data indicates that effective chemical structures all reduced the quantity of C 40-50 molecular weight waxes contained in the resulting paraffin deposits.

Economides et al. [3] The rheological properties of Prudhoe Bay oil, as with any other mixture of hydrocarbons, are markedly affected by the lowering of temperature. The Trans Alaska pipeline traversing the state in a North/South direction is subjected to severe ambient temperatures during the winter months. A prolonged flow interruption would result in inevitable heat losses from the trapped crude oil. The temperature decline would cause a significant alteration of the flow behavior. A fundamental heat transfer study and laboratory measurements were combined in order to forecast the rheological response and subsequent start-up requirements of Prudhoe Bay oil in gathering lines and in the Trans Alaska pipeline.

Yan et al.[4] An extensive study of the rheological characteristics of crude oil is indispensable for lowering the energy consumption and ensuring safety and cost effectiveness in pipeline transportation of waxy crudes. The relative amount and molecular distribution of wax, resin, and asphaltene in a high-pour-point waxy crude directly affect the rheological properties of crude oil. Phase changes are observed

under various thermal conditions. At an elevated temperature, wax dissolves in crude oil to form a homogeneous fluid. When the temperature is lowered, wax crystals separate out with adsorbed resin and asphaltene, and crude oil turns from a liquid to a suspension. With further temperature reduction, a continuous phase of wax crystal lattice is formed, while liquid hydrocarbon becomes a dispersed phase. Crude oil then loses flow ability, displaying conditional freezing. This phase change causes crude oil to deviate from Newtonian behavior and to exhibit shear thinning, thixotropy, and structural strength. With continuous lowering of the temperature, waxy crude can be changed rheologically from a Newtonian fluid into pseudo plastic, thixotropic/pseudo plastic, and thixotropic/ yield-pseudo plastic fluids successively. This change in rheological types can be attributed to the thermal and shear histories, as well as to the composition of crude oil. This paper focuses on the rheological properties of Daqing crude oil on the basis of experimental work.

Argillier et al. [5] The increasing oil demand is leading to the development of the very large world resources of heavy oils that are of the same order of magnitude than conventional oils. However, production and transport of these oils are challenging because of their very high viscosities. The aim of this study was first to understand the role of asphaltenes in these high viscosities and secondly to evaluate the viscosity reduction efficiency when blending with different diluents. Many previous works studied asphaltene associations in simple organic solvents like toluene or toluene/heptane mixtures, but these conditions are not representative of heavy crude oils. The approach has been to characterize the rheological behavior of asphaltenes in their natural environment. Samples coming from the same crude oil have been prepared with different asphaltenes contents, from 0 to 20%, after deasphaltating and recombination. From viscosity measurements two concentration

regimes were identified: a diluted regime where the apparent viscosity increases linearly with the weight fraction of asphaltenes and a concentrated regime where the viscosity increases dramatically because of asphaltene particles entanglement. The diluted regime can be described as a solution of solvated asphaltene particles that are independent from one another. Natural heavy crude oils correspond to the concentrated regime and the high viscosities observed are due to this entanglement of solvated asphaltene particles. A strong influence of temperature on the rheology is revealed by measured high activation energies. Dilution of heavy oils has been studied using various solvents, in terms of aromaticity, chemical nature and viscosity. Dilution with low viscosity hydrocarbons, like light crude oil or naphtha, has shown that the viscosity reduction efficiency is controlled by the sole viscosity of the diluent and not by its aromaticity. The aromaticity has no effect up to very high dilution rate, more than 60%, where flocculation may begin. Results have also shown that blending diluents of different chemical natures and polarities can enhance viscosity reduction. From these observations, the colloidal description of heavy oils can be extended to diluted heavy oils, considered as solutions of asphaltene particles solvated in diluted maltenes.

Hénaut et al. [6] Heavy oils represent a strategic source of hydrocarbons as their reserves are of the same order of magnitude as the ones of conventional oils. The production of these crudes remains low, in particular because of their very high viscosities. The asphaltene they contain are known to be responsible for this situation. Actually, many studies have shown that these high molecular weight polar components self associate more or less severely depending on different parameters like temperature, concentration and solvent quality. The experimental work was usually performed using simple organic solvents (toluene, heptanes. etc) which are

not representative of complex heavy crude oils. Therefore, it was decided to investigate the rheological behavior of asphaltenes in their natural environment and in relation with their structure. Samples coming from the same crude oil were prepared with different asphaltenes contents, from 0 to 20% in weight. The apparent viscosity and the oscillatory modulus (G' and G") were measured with a controlled stress rheometer. Two domains were identified. The first one concerns the dilute samples for which the relative viscosity increases linearly with the weight fraction of asphaltenes. In this domain, the aggregates of asphaltenes stay independent from one another and have the same radius of gyration. For the more concentrated samples, the viscosity increases dramatically because of the aggregates entanglement. Concerning the oscillatory experiments, the elastic character increases from the first domain to the second one, which confirms that a structural change occurs combining the rheological measurements reveals an analogy between heavy crude oils and concentrated colloidal systems of polymer solutions. All these results help the understanding of the flow properties of heavy crude oils and aim to contribute to the improvement of their transport.

Khan et al. [7] Empirical equations for estimating viscosity: above, at, and below the bubble point pressure were developed based on data from Saudi Arabian crude oils. Both statistical and graphical techniques have been employed to evaluate these equations as compared to other published crude oil viscosity correlations using the same data. It is shown that the developed correlations provide more accurate estimates of viscosity in all three regimes of pressure.

Wardhaugh et al. [8] Crude oils from China, Australasia and many other parts of the world, containing waxy crystals and colloidal asphaltenes, possess distinct non-Newtonian flow properties which depend strongly on the shear and thermal history

and result in special difficulties being encountered in all types of viscometers. Experimental techniques are discussed which allow reproducible equilibrium data to be obtained in the concentric cylinder and the cone and plate viscometers. The shear history dependence of the flow properties, which is shown to occur in both Australasian and Chinese crudes, alters the conventional design and scale-up assumptions. Flow in a capillary or pipeline is shown to be a composite effect of the range of shear rates that occurs across the radius of the pipe. An identical composite effect must occur for the scale-up assumption to remain valid. Pipeline flow can be determined from laboratory data by modified design techniques, which also allow the quantitative assessment of oil treatment methods. A lower limit to pipeline operation, due to the shear history effect, is shown to exist, which has an effect on the assessment of oil treatment methods and on the operation of declining oil fields.

Argillier et al. [9] Because of very important reserves that are of the same order of magnitude as conventional oils, heavy oils represent a strategic source of hydrocarbons. The major difficulty for producing and transporting these crudes comes from their very high viscosities. The success of exploitation of these petroleum products requires new treatments to improve their transport. Such a target implies to better understand the relationship between the compositions of heavy oils, in particular in terms of asphaltenes and resins content and their flow properties. Influence of asphaltenes content in the crude has been particularly studied in the lab: the experimental work revealed the existence of a critical concentration C* above which the asphaltene particles overlap. This structural change dramatically increases the viscosity and intensifies the elastic character of heavy crude oils. A further series of experiments has focused on the influence of resins: they show that in dilute regime (C<C*), resins increase the viscosity of the crude and in concentrated regime

(C>C*), which corresponds to the case of a heavy oil, they lower the asphaltenes effect on viscosity. Experiments were first carried out with asphaltenes and nonylphenol as a model of resins and followed by experimental work on real crude that confirmed the trends. To understand the rheological behavior of a heavy crude oil in relation with its internal structure, asphaltenes and resins have to be simultaneously considered. This study concluded that the origin of the high viscosities of heavy oils comes from to the entanglement of solvated asphaltene particles stabilized by resin molecules. A strong influence of temperature on the rheology is also revealed by high activation energy measurements. This thermal dependent rheological behavior shows that the internal organization of the heavy crude oil is partly based on thermal dependent physical bonds. Using the reversibility of these physical links, we should be able to modify the structure of heavy crude oils to facilitate their transport.

Sharma et al. [10] The heavy oil belt of North Cambay Basin comprising of Santhal, Lanwa and Balol oil fields poses great problems in floatation of these heavy oils due to high viscosity (10,000-16,000 cPs) of the emulsion. Oil-in-water emulsions provide a cost-effective alternative to the heated pipelines or diluents for their transportation. Emulsions in different phase ratios and application doses of 2000-5000 ppm of non-ionic surfactants have been found to be effective in phase reversal of emulsions with drastic reduction in viscosities, which are in 100-400 cPs range at pipeline operating conditions. Non-ionic surfactants have the advantage of relative insensitivity to the salt content of the aqueous phase. The non-ionic family of surfactants has been used successfully for the formation of stable emulsions that resist inversion to a wide operating temperature range. The reverse emulsions are heat sensitive and resolve themselves at elevated temperatures without addition of dehydration chemicals. Suggested surfactant treatment has the potential to

successfully transport heavy/viscous emulsions of Lanwa oilfield resulting in tremendous savings in transportation costs.

Ajienka et al. [11] Waxy crude oils are difficult to handle. They exhibit non-Newtonian flow behavior at temperatures below the cloud-point because of wax crystallization. On further cooling and successive crystallization, gelling occurs below the critical pour point. Wax precipitation results in handling problems and increased production costs. Despite these problems waxy crudes are of economic importance because of their lightness, low sulphur content and the considerable reserves worldwide.

In order to accurately predict flowing and static temperature profiles, design waxy crude oil pipelines, evaluate flow interruption scenarios and startup requirements in the handling of waxy crude oils, the effect of temperature on the rheology of waxy crude oils must be determined. This was investigated for six waxy crude oils produced by different Nigerian oil fields. Temperature ranges defining both Newtonian and non-Newtonian flow regimes were covered. The range of API gravity covered was 22-28 degrees while that of pour point was 85-100 degrees F.

Waxy crude oils are not only temperature dependent but are also shear rate dependent and exhibit thixotopy. Generally, flow behavior is Newtonian above the cloud-point and between the cloud-point and pour point, crude oil is pseudoplastic or thixotropic/pseudoplastic and at temperatures below the pour point, they exhibit thixotropic/yield pseudoplastic behavior. Based on these studies, empirical correlations of rheological parameters as functions of normalized temperature and API gravity were obtained. The parameters correlated for the non-Newtonian flow regions are power law flow parameters: flow behavior index, flow consistency index, and yield stress and Casson fluid model parameter. For the Newtonian region,

apparent viscosity is correlated. The results show that with the exception of flow behavior index, these parameters are strongly temperature dependent.

1.2 Paraffin Deposition in Crude Oil Transporting Pipelines

Jessen et al. [12] Conducted experiments and observed that as velocity increases deposition increases up to the transition from laminar to turbulent flow from which point onwards it starts decreasing. They explained this by proposing the presence of higher mass transfer coefficient at higher flow rates and a sloughing effect due to viscous drag exceeding the shear stresses within the deposited wax. They also observed increased deposit hardness at increasing flow rates. They also proposed two mechanisms of paraffin deposition: deposition of paraffin from crude oil at the pipe walls (molecular diffusion) and particle transport to the wall, with the observation that molecular diffusion seems controlling.

Hunt. [13] Conducted a paraffin deposition study using flow and cold-spot apparatuses. He observed the mechanism of deposit growth by diffusion of paraffin molecules from solution to be consistent with lab and field measurements. He also noted that as deposit thickness increases the shearing force on it increases and may become sufficient to tear it loose (sloughing). Hunt also noticed that it was not possible to form deposits under constant temperature.

Bott et al. [14] Studied the fluctuating nature of heat transfer resistance of fouled heat exchanger tubes due to paraffin deposition upon cooling. They observed that during the deposition process heat flux decreases (due to insulation and fall in bulk oil temperature) and shear stress increases (due to reduced diameter). They noted that as the wax thickness reaches a critical value it begins to fail. They attributed the fluctuating nature of the heat transfer resistance to this buildup and removal of

foulant. They also observed that flow rate and temperature decrease the number of particles able to deposit while greater wax concentration increases it.

Drayer et al. [15] A novel process for the pipeline transportation of high pour point, highly paraffinic crudes has been developed. The process involved formation of hydrocarbon slurry after distillation of the crude into two fractions. Small, solid particles of the heavy fraction were formed and dispersed in the light liquid fraction. Experimental flow data for these non-Newtonian slurry systems have been scaled to commercial-size pipelines. The process has been adapted also to several shale oil systems.

Burger et al. [16] investigated the mechanisms of wax deposition in the Trans Alaska pipeline. In a well-drawn study they conducted lab, field experiments and proposed a mechanistic model. They emphasized on molecular diffusion and shear dispersion as the two main deposition mechanisms and at the same time discounted Brownian diffusion and gravity settling. For turbulent flow, the region of activity was identified to be localized in the laminar sub-layer. For particle transport, the rate of incorporation of particles at the solid/liquid interface was thought to be rate limiting and was expressed by a first order rate equation directly proportional to the shear rate and average particle-wax concentration. The rate constant was determined by parameter fitting deposition rates over a range of deposition conditions and averaging to arrive at a single number. Their model predictions matched field data obtained by them fairly well. From their calculations, at low heat fluxes, shear dispersion was found to dominate whereas at high heat fluxes molecular diffusion seemed to play the critical role. At zero heat fluxes, they found, like others before them [13], no deposition. They hinted at the possibility of a sloughing mechanism being at play. They also proposed the immobile deposit at the wall to be a porous structure with

pore spaces filled with liquid oil. They measured the average wax content of the deposit to be around 14 to 17%. They further pointed out that the deposit formed under favorable conditions is only a small fraction of the actual precipitate, which in turn is just a fraction of the potentially precipitable hydro carbonaceous material in the oil.

Weingarten et al. [17] Measured the deposition rates by diffusion and also studied the effect of shear on deposit volume using a set of ad hoc flow setups. As per their observations, both shear transport and diffusion play a definite role in wax deposition. Also, upon normalizing the temperature effect (diffusion) out, the deposition rates were found to increase linearly with shear rate, as proposed by Burger et al. [16] earlier. However, at a critical shear rate (2450 1/s, in their case), when the shear stress at the edge of the deposit reaches its shear strength, the rate of total deposition was found to approach zero. The sloughing rate was not quantified. However, they observed in their experiments that sloughing had no relation with the turbulence of the flow. As long as the wall shear stress exceeded the deposit strength, waxes would be sloughed off even if the flow were laminar. This contradicts the findings by Jessen et al. [12], who placed an emphasis on the transition from laminar to turbulent for the onset of sloughing. Also, in the absence of a temperature gradient, despite the oil temperature being below the crystallization temperature, they observed no deposition too.

Majeed et al. [18] Studied wax deposition for North Sea oils in a lab flow line at laminar flow and developed a model based on molecular diffusion only. Diffusion contribution of each individual diffusing species was summed to obtain the overall deposition rate. However, diffusivity was assumed to be the same for all species. Crystal diffusion was thought by the authors to be away from the wall and its effect

was presumed to reduce the overall deposition rate. This mechanism was however not included into the model. Their estimates for wax deposition reasonably agree with experiments at high heat fluxes and only for short deposition times. They rationalized the under prediction by their model at low heat fluxes to be due to the absence of the shear dispersion term. Some of their offshore field data suggest trends similar to the results of Jessen et al. [12], where the deposition rates at low heat flux first increase with flow rate and then begin to decrease. However, the point of maxima doesn't seem to necessarily lie in the neighborhood of the transition from laminar to turbulent.

Svendsen [19] Performed a detailed mathematical analysis of the deposition problem for both open and closed pipeline systems. He obtained deposition as a function of time by solving differential equations derived from the principles of mass and energy conservation and the laws of diffusion. Particle transport and sloughing were not considered. From his calculations, Svendsen inferred that wax deposition could be considerably reduced even when the wall temperature is below the cloud point, provided that the liquid/solid phase transition expressed by the change in moles of liquid with temperature is small at the wall temperature. Another point made was that if the coefficient of thermal expansion is sufficiently large some components may separate and move in opposite radial directions at temperatures below the cloud point.

Brown et al. [20] Confirmed in their flow apparatus that at zero heat flux no deposition takes place. They also observed a reduction in deposition tendency over an increase in shear rate from 330 1/s to 1330 1/s. Unlike Weingarten et al. [17] before them, no initial period of deposit increase with shear rate was observed. Thus also, their results failed to emulate the shear rate dependence of the particle incorporation mechanism of Burger et al [16]. Based on the above two observations, they concluded that shear dispersion does not contribute to paraffin deposition. Sloughing though

observed was not ventured into further. Only molecular diffusion was modelled as a deposition mechanism. The proportionality constant from the expression for diffusivity was used as a fitting parameter to numerically match the prediction trend to the experimental data. Furthermore, the deposits formed at higher shear rates were noted to be hard and brittle while those at low shear rates were noticed to be soft and pliable. They explained that this was to be due to a decrease in trapped oil content of the gel deposit at higher shears. Based on their prediction for start-up deposition rates, they also concluded that start-ups are not expected to present significantly greater deposition problems than steady-state operations.

Hsu et al. [21] Analyzed wax deposition of waxy live crudes in a high-pressure turbulent flow loop. They too observed that wax deposition is negligibly small when the heat flux across the wall is small or negative. Their experiments showed that wax deposition occurs only when the temperature of the deposition surface is lower than the cloud point - irrespective of the average oil temperature. They also found the sloughing effect to be significant enough for turbulent flow to be ignored in modeling. Their work also demonstrated an increase in wax hardness and carbon number of the deposit with retention time.

Hamouda et al. [22] Experimentally found out that though gravity settling contributes to the total deposition mechanism, it does so to a lesser extent than shear dispersion, and molecular diffusion. Of these last two, molecular diffusion seems controlling and shear dispersion becomes important only at low temperature gradients. They found wax deposition to be negligible under near about zero heat flux conditions. They also observed for their paraffin the start of sloughing at 3500 1/s and no deposition at 5500 1/s. To account for this behavior in their model they introduced the ’paraffin adhesion constant’, which multiplies the overall deposition rate (which is

the sum of molecular diffusion and shear dispersion). The value of this constant was set to be one at 35001/s and zero at 55001/s.

Creek et al. [23] Performed experiments in a pilot scale deposition facility at Tulsa. Once again, they too noticed no deposition under zero heat flux conditions. Plus, they noticed an increase in deposit thickness with an increase in transverse temperature difference. Thus, they qualified molecular diffusion as the dominating deposition mechanism and ignored shear dispersion. Deposits were found to be harder for turbulent flow and for lower transverse temperature differences. The former was attributed to lower oil content at higher flow rates. The deposition in turbulent flow was found to be far less than in laminar flow. In the same vein, deposition rates were found to decrease with increasing flow rates. A sloughing mechanism was suggested to be the cause for this. They also observed aging only in turbulent flow, not in laminar flow. The explanation put forth by the authors was the presence of a greater heat flow due to a lesser insulation effect of the thinner deposits at high flow rates. Also, Ostwald ripening was proposed as the possible aging mechanism.

Singh et al. [24] Conducted laminar flow experiments in a lab flow loop and primarily studied the aging phenomenon. They also developed a mathematical model to describe the wax deposition in their flow-loop apparatus that matched their experimental results fairly accurately. For laminar flow, they experimentally verified the absence of shear removal, mechanical compression and particulate deposition. They identified the aging process to be a counter diffusion process with oil diffusing out and wax diffusing into the deposit with time. They found the aging of the gel deposit (the increase in its wax content) to be a strong function of the temperature difference across it. They used the term critical carbon number to delineate solute wax from solvent oil. For the model oil used by them they found the critical carbon

number to be 29. They observed the wax deposit to be thinner at higher flow rates. This was reasoned to be due to a shorter growth period and slower growth rate, since the interface temperature reaches the cloud point faster at higher flow rates. Decreased thicknesses were observed at higher wall temperatures.

Nazar et al. [25] Presented a model for both laminar and turbulent flows. Experiments were conducted for laminar flow only. For fully developed temperature profiles in turbulent flow only molecular diffusion was used as a deposition mechanism and a sloughing term was modeled for removal kinetics. For laminar flow, the amount of wax deposited was found to increase with increasing flow rate. In turbulent flow, their simulations showed presence of a critical flow rate above which the sloughing term starts decreasing the overall deposition rate. The sloughing term was concluded to be important for turbulent flow. A recurrent theme is the absence of deposition in pipes under zero heat flux conditions even if the oil temperature is below the bulk temperature. In the absence of a temperature (and thus concentration) gradient, diffusion, here, becomes equal to zero. The remaining two deposit mechanisms are particle transport and sloughing. Such a result could only imply either absence of particle transport or its balance by an equivalent sloughing force.

As can be seen from the above literature review, though a lot of labs have observed negligible depositions, none is too explicit in providing an exact reason. If particle transport as a deposition mechanism is absent for this case, and then it would be absent even when the pipeline is losing heat. However, if a shearing force here is just balancing it, then a change in conditions could bring it to the forefront making its effect directly felt on the wax thicknesses. In any case, future-modeling attempts will be directly affected.

In this Dissertation the rheological properties of transported crude oil have been evaluated. A mathematical model of wax deposition in pipelines has been developed. Selected results from the wax deposition have been used for determining the economic interval for the pigging of the pipeline.

CHAPTER 2
HISTORY OF THE ALGYO-KISKUNHALAS-SZAZHALOMBATTA PIPELINE

Crude oil is transported through this pipeline system from two different fields; the first transporting line starts from Algyo and ends in Szazhalombatta, where the refinery is located. This line has been held under operation since 1970, with a 163 km length, 308mm, 324mm internal and external nominal diameters and 8mm pipe thickness at conjunction, otherwise 5mm thickness. The second transporting line starts from Kiskunhalas-Szank with a 39 km length, 300 mm, 304 mm nominal diameters and started to operate in 1979.

Both of the above mentioned pipelines join each other at Palmonostora 42 km from Algyo, 39 km from Kiskunhalas, flowing pattern considered as steady state flow regardless of height differences. The transported crude oils have Non-Newtonian pseudoplastic behavior. Mixing of crude oil with gasoline reduces the pressure drop, the amount of gasoline used depends on external temperature. In winter when temperature falls, more gasoline is used. Algyo's crude oil has a density of 797 kg/m^3 and Kiskunhalas's crude oil 849 kg/m^3, and the mixing of both 802 kg/m^3, the water content of the different crude oils is as follows: -

Algyo	0.14 W %
Mixture	0.16 W%

The pressure needed for pumping is maintained by two pump stations, the first is located in Algyo, and the second in Kiskunhalas. The pipeline crosses the Danube

River at a distance of 154 km, and 159 km respectively and reaches the final destination in Szazhalombatta.

Three pigging stations are installed along the pipeline; the first one is located at the starting point (Algyo), the second one in Kecskemet, and the third in Szazhalombatta.

Algyo-Szazhalombatta consists of 10 sections, and Kiskunhalas Palmonostora consists of 2 sections, the average laying depth of pipeline is 1.5m

Data and the elevation of pipeline profile is shown in the following tables and Figures

Table 1-1 Algyo-Szazhalombatta transporting pipeline

Location	**Distance (km)**	**Geodetic height (m)**
Algyo	0.0	80.40
Sovenyhaza	25.585	86.40
Kiskunfelegyhaza	49.624	92.60
Kecskemet	78.878	114.50
Lajosmizse	99.037	140.20
Pusztavacs	113.220	128.40
Ocsa	137.615	97.45
Majoshaza	153.901	100.86
Szigetcsep	154.557	99.90
Tokol	159.137	100.80
Szazhaombatta	161.360	143.62

Table 1-2 Kiskunhalas-Szank-Palmonostora pipeline

Location	**Distance (km)**	**Geodetic height (m)**
Kiskunhalas	0.0	123.70
Szank1	18.304	109.66
Szank2	18.333	109.85
Palmonostora	38.962	88.50

Fig. 1-1 Algyo-Szazhalombatta pipeline profile.

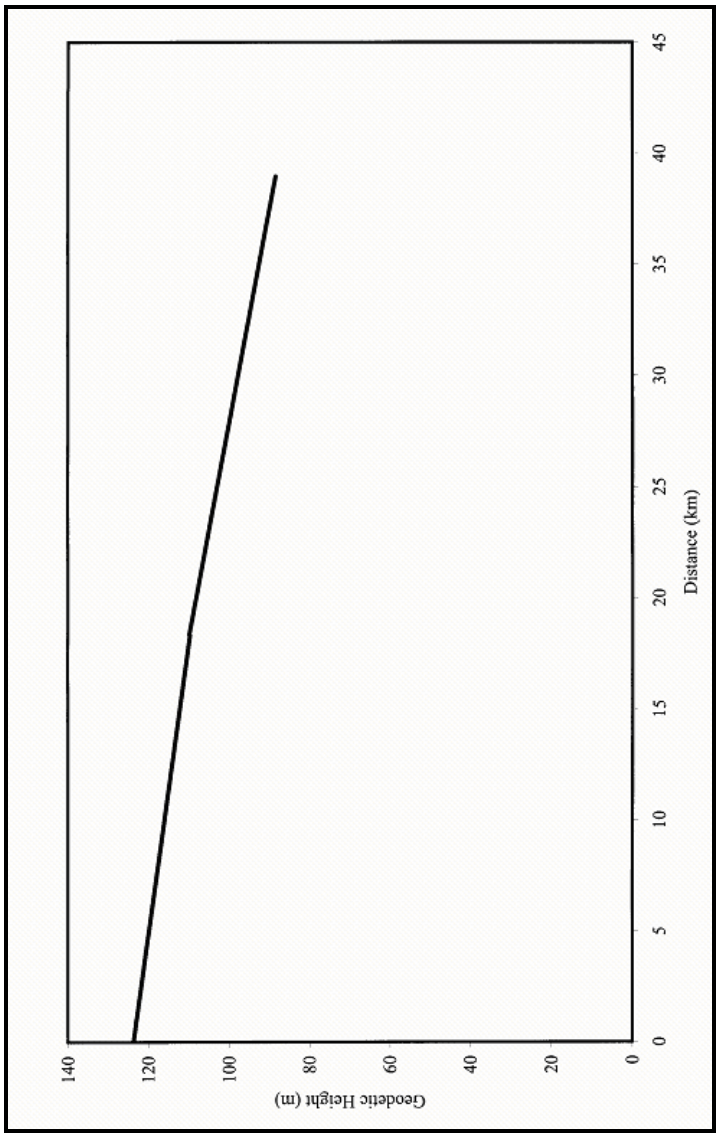

Fig. 1-2 Kiskunhalas-Palmonostora pipeline profile.

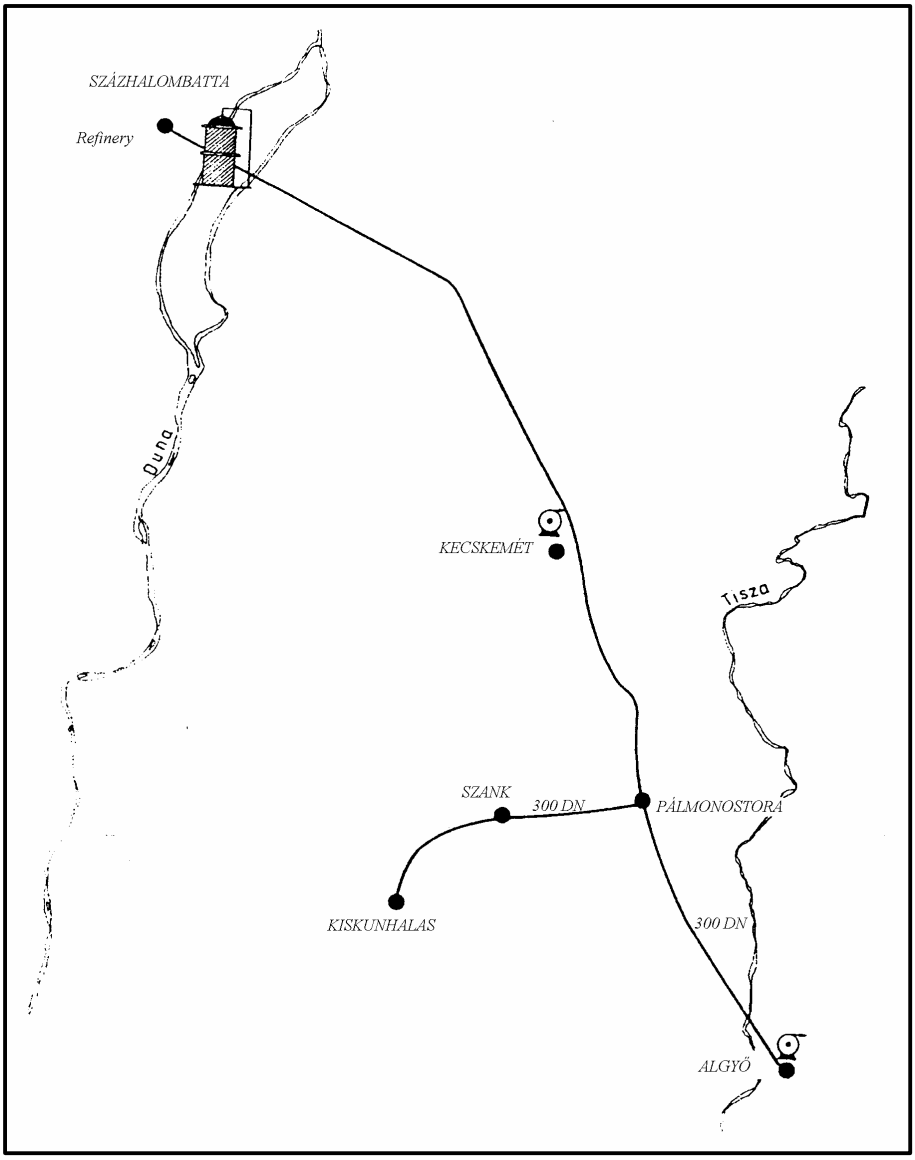

Fig. 1-3 Algyo-Szazhalombatta pipeline location.

CHAPTER 3
RHEOLOGICAL PROPERTIES OF ALGYO AND KISKUNHALAS CRUDE OILS

3.1 Introduction

Fluids such as water, air, ethanol, and benzene are Newtonian. This means that a plot of shear stress versus shear rate at a given temperature is a straight line with a constant slope that is independent of the shear rate. We call this slope the viscosity of the fluid. All gases are Newtonian. Also, low molecular weight liquids, and solutions of low molecular weight substances in liquids are usually Newtonian. Some examples are aqueous solutions of sugar or salt.

Any fluid that does not obey the Newtonian relationship between the shear stress and shear rate is called Non-Newtonian. The subject of “Rheology” is devoted to the study of the behavior of such fluids. High molecular weight liquids which include polymer melts and solutions of polymers, as well as liquids in which fine particles are suspended (slurries and pastes), are usually non-Newtonian. In this case, the slope of the shear stress versus shear rate curve will not be constant as we change the shear rate. When the viscosity decreases with increasing shear rate, we call the fluid shear thinning. In the opposite case where the viscosity increases as the fluid is subjected to a higher shear rate, the fluid is called shear thickening. Shear-thinning behavior is more common than shear thickening. Shear-thinning fluids also are called pseudoplastic fluids. A typical shear stress versus shear rate plot for a shear-thinning fluid looks like the following Figure. [26]

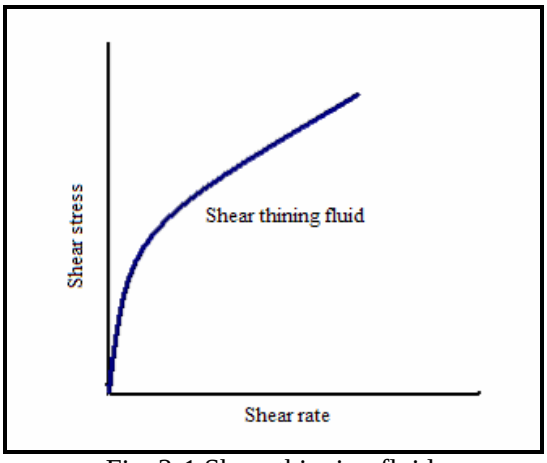

Fig. 3-1 Shear thinning fluid.

3.2 Properties of Non-Newtonian Fluids

There are many fluids known as Non-Newtonian fluids for which the viscosity depends on the shear rate on the fluid. The behavior of these fluids can be represented well by a graph (referred to as a flow curve) of shear stress (τ) versus shear rate (du/dr) as below. [27]

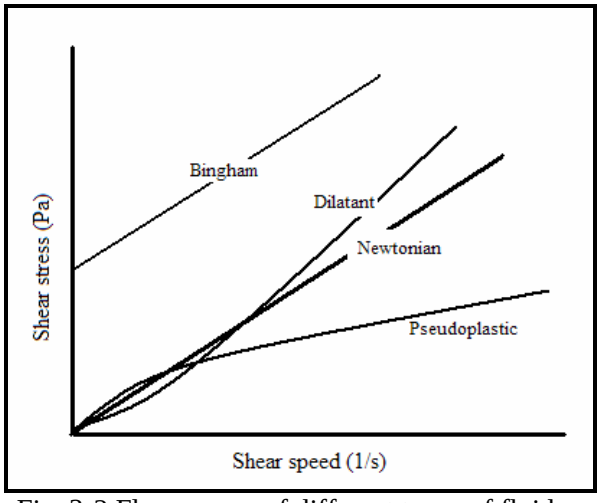

Fig. 3-2 Flow curves of different types of fluid.

Non-Newtonian fluids are divided into different categories:

1. Time independent Fluids (Purely viscous fluids)

- Bingham (plastic) fluid behaves as a solid until a critical shear rate is achieved, e.g., drilling mud and grain.
- Pseudoplastic fluids Viscosity decreases as the shear rate is increased, e.g., polymeric solutions, paints, mayonnaise, paper pulp.
- Dilatant fluids: viscosity increases as the shear rate is increased, e.g., high solids content solutions of starch and sand.

2. Time Dependent fluids:
   - Thixotropic fluids: viscosity decreases with time of shearing e.g., paint, margarine, and honey.
   - Rheopectic fluids: viscosity increases with time of shearing.
   - Viscoelastic fluids show some elastic behavior, e.g., jelly.

The equation, which relates the shear stress to the shear rate is called a "constitutive equation". Pseudoplastic and dilatants fluids can be modeled by the Power Law equation.

$$t = -K\left(\frac{du}{dr}\right)^n \qquad (3\text{-}1)$$

Where:

t : shear stress (Pa)

K: consistency index found from flow curves.

$\left(\frac{du}{dr}\right)$: shear speed (1/s)

n : rheological index.

Both of K and n can be obtained from the rheological measurement and depend on fluid temperature.

3.3 General Equations for Non-Newtonian Fluids

Assumptions are the following:

1. Fluid velocity is zero at the wall
2. Fluid streamlines are parallel to wall and there is no circumferential flow
3. The hydrostatic pressure is uniform across any radial section
4. Flow is viscometrical, i.e., does not change with time.
5. Entrance and exit effects are ignored.

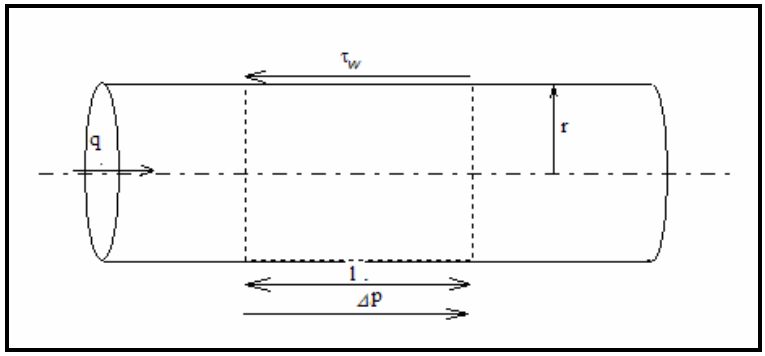

Fig. 3-3 Components of a force balance.

From a force balance:

$$t_w 2p.rl - \Delta pp.r^2 = 0 \tag{3-2}$$

Where: t_w *is* the wall shear stress and R is the pipe radius. Hence

$$t_w = \frac{d_i \Delta p}{4l} \tag{3-3}$$

Note that this equation assumes only circular pipe.

Further we can show that

$$\frac{q}{p.r^3} = \frac{1}{t_w^3} \int_0^{t_w} t^2 f(t) dt \tag{3-4}$$

Where *f (t) = -du/dr*. This then is a generalized equation relating flow to shear stress.

and further after some integration and manipulation

$$\left(-\frac{du}{dr}\right)_w = \frac{8v}{d_i}\left[\frac{3}{4}+\frac{1}{4n'}\right] \tag{3-5}$$

Where:

$$n' = \frac{d\left(\ln\left(\frac{d\,?\,p}{4l}\right)\right)}{d\left(\ln\left(\frac{8u}{d}\right)\right)} \tag{3-6}$$

i.e., n' is the slope of a graph of *dDp/4l* vs. *8u/d*.

This equation shows that it is possible to write

$$\frac{d_i\,?p}{4l} = t_w = K\left(\frac{8u}{d_i}\right)^{n'} \tag{3-7}$$

We see here a similarity in form to the Power Law equation, $t = -K\left(\frac{du}{dy}\right)^n$ but in this derivation we have made no assumptions about the "constitutive equation" for the fluid.

The two constants K and n' can be used for prediction of pressure drop in turbulent systems. [27]

3.3.1 The Method of Dodge and Metzner

Dodge and Metzner used the generalized Reynolds number defined by Metzner and Reed (1955) who noted that a time-independent fluid in laminar tube flow could be adequately modeled by:

$$t_w = K\left(\frac{8u}{d}\right)^n \tag{3-8}$$

where K' and n' need not be constant. They defined the generalized Reynolds number, Re_g, so that under laminar flow

$$f = \frac{16}{\mathrm{Re}_g} \tag{3-9}$$

Thus it can be shown that

$$\mathrm{Re}_g = \frac{d^n u^{2-n} r}{K 8^{n-1}} \tag{3-10}$$

Or

$$N_{\mathrm{Re}\,pp} = \frac{d_i{}^n u^{(2-n)} r}{\frac{K}{8}\left(6+\frac{2}{n}\right)^n} \tag{3-11}$$

And this is the Reynolds number for the Non Newtonian pseudoplastic fluids.

3.3.2 Derivation of the BNS equation

Considering the steady state, one-dimensional axisymmetric turbulent flow in a circular, infinitely long pipe and a cylindrical coordinate system is chosen, the momentum equation for this case is

$$\frac{rgJr}{2} + K\left|\frac{dv}{dr}\right|^{n-1}\left(\frac{dv}{dr}\right) - r\overline{u'w'} = 0 \tag{3-12}$$

Where:

$$K\left|\frac{dv}{dr}\right|^{n-1}\left(\frac{dv}{dr}\right) = t$$

$$K = m\left(\frac{dv}{dr}\right)^{1-n}$$

$\rho\overline{u'w'}$:is the τ'_{rz} component of the turbulent stress tensor.

g :Gravity m/s^2

r : Density (kg/m^3)

J: Hydraulic gradient

r: Radius of laminar sublayer (m)

K: consistency index

n: behavior index.

m : Apparent viscosity (N/m^2s)

Both of K and n depend on the fluid temperature.

The solution of this differential equation can be done into two parts in accordance with the nature of flow. The flow near the wall is laminar within a very thin laminar sublayer. Turbulent momentum transfer cannot be developed here. Since the thickness of the laminar sublayer δ is very small relative to the radius of the pipe *R*, the velocity distribution within the laminar sublayer may be taken as linear. This is equivalent to their existence a uniform shear stress in the sublayer equals to the wall-shear stress τ_R. Thus, we can write

$$\frac{\rho g J R}{2} - K\left|\frac{dv}{dr}\right|^n = 0 \tag{3-13}$$

The definition of the friction velocity

$$v_* = \sqrt{\frac{gJR}{2}} \tag{3-14}$$

can be used, so that we obtain

$$-\frac{dv}{dr} = \left(\frac{v^2{}_* ?}{K}\right)^{\frac{1}{n}} \tag{3-15}$$

The linearizerd velocity profile within the laminar sublayer can be expressed in dimensionless form:

$$\frac{v}{v_*} = v_*^{\frac{2-n}{n}}\left(\frac{r}{K}\right)^{\frac{1}{n}}(R-r) \tag{3-16}$$

Outside the laminar sublayer, the viscous shear stresses are negligible small compared to the turbulent stresses. Applying Karman's equation for the mixing length the momentum equation is obtained as

$$\frac{rgJr}{2} = -rk^2 \frac{\left(\frac{dv}{dr}\right)^4}{\left(\frac{d^2v}{dr^2}\right)^2} \tag{3-17}$$

Dividing both sides by density, taking the square root of the last equation and multiplied by R/R, the equation will be as the following:

$$-v_* \sqrt{\frac{r}{R}}\, k \frac{\left(\frac{dv}{dr}\right)^4}{\left(\frac{d^2v}{dr^2}\right)} \tag{3-18}$$

Taking the reciprocal of both sides we have:

$$-\frac{\left(\frac{d^2v}{dr^2}\right)}{\left(\frac{dv}{dr}\right)^2} = \frac{k}{v_*}\sqrt{\frac{R}{r}} \quad , \tag{3-19}$$

which can readly integrated. After integration we obtain:

$$\frac{1}{\frac{dv}{dr}} = \frac{2k}{v_*}\sqrt{Rr} + K_1 \tag{3-20}$$

In order to determine the integration constant K_1 we may prescribe as a boundary condition that the velocity gradient at wall becomes infinite:

$$\left(\frac{dv}{dr}\right)_{r=R} = \infty$$

This assumption is permitted since it is outside the validity interval of the solution.

Thus:

$$K_1 = \frac{2k\ R}{v_*}$$

Substituting the constant K_1, the following expression is obtained:

$$\frac{1}{\left(\frac{dv}{dr}\right)} = -\frac{2kR}{v_*}\left(1-\sqrt{\frac{r}{R}}\right)$$

Taking the reciprocal of both sides and integrating yields

$$v = \frac{v_*}{k}\left[\sqrt{\frac{r}{R}} + \ln\left(1-\sqrt{\frac{r}{R}}\right)\right] + K_2 \qquad (3\text{-}21)$$

Now we need one more boundary condition to determine the integration constant K_2. It is a known experimental fact that the maximum of the velocity distribution is at the pipe axis. Therefore, at r=0,v=v_{max}, thus K_2=v_{max}.

Thus we obtain the following dimensionless velocity profile:

$$\frac{v_{\max} - v}{v_*} = \frac{1}{?}\left[\sqrt{\frac{r}{R}} + \ln\left(1-\sqrt{\frac{r}{R}}\right)\right] \qquad (3\text{-}22)$$

This relation offers a good description of the velocity profile, but does contain v_{max} as unknown arbitrary additional term. It is obvious that the velocities are equal on both sides of the surface which forms the boundary between the turbulent core flow and the laminar sublayer adjacent to the wall. Thus the turbulent velocity profile must match that of laminar sublayer at the position $r = R - d$, i.e.

$$\frac{v_* d}{n} = \frac{v_{\max}}{v_*} + \frac{1}{k}\left[\sqrt{\frac{R-d}{R}} + \ln\left(1-\sqrt{\frac{R-d}{R}}\right)\right] \qquad (3\text{-}23)$$

A very important observation of Prandtl is that

$$\frac{\boldsymbol{v}_* d}{n} = a = \text{constant}.$$

Since $d/R \langle\langle 1$ the following approximations based on the binominal theorem are convenient:

$$\sqrt{1-\frac{d}{R}} \approx 1$$

And $$\ln\left(1-\sqrt{1-\frac{d}{R}}\right) \approx \ln\left[1-\left(1-\frac{d}{2R}\right)\right] = \ln\frac{d}{2R}$$

After substitution the maximum velocity is obtained as

$$\frac{v_{\max}}{v_*} = \left(\frac{v_*^{2-n} r}{K}\right)^{\frac{1}{n}} d - \frac{1}{k}\left(1+\ln\frac{d}{D}\right) \qquad (3\text{-}24)$$

To calculate the maximum velocity it is necessary that δ be known. Prandtl assumed that for a Newtonian fluid

$$\mathrm{Re}_\delta = \frac{v_* \rho}{\nu} = \cos t\,.$$

Analogously, we assume that for pseudoplastic fluids

$$\mathrm{Re}_{pd} = \frac{v_*^{2-n} d^n r}{\frac{K}{8}\left(6+\frac{2}{n}\right)^n} const \qquad (3\text{-}25)$$

where:

d : thickness of laminar sublayer instead of pipe diameter.

Using this equation and the Reynolds number for non Newtonian pseudoplastic fluids derived by Metzner and Reed (1955):

$$\mathrm{Re}^*_p = \frac{v^{2-n} d^n r}{\frac{K}{8}\left(\frac{6n+2}{n}\right)^n} \qquad (3\text{-}26)$$

$$\delta = \left(\frac{\mathrm{Re}_{p\delta}}{\mathrm{Re}_p}\right)^{\frac{1}{n}} \left(\frac{c}{v_*}\right)^{\frac{2-n}{n}} D \qquad (3\text{-}27)$$

Substituting this into

$$\frac{v_{max}}{v_*} = \frac{1}{n\kappa}\ln\left[\mathrm{Re}_p\left(\frac{v_*}{c}\right)^{2-n}\right] - \frac{1}{\kappa}\left(1 + \frac{\ln \mathrm{Re}_{p\delta}}{n}\right) + \frac{6n+2}{n}\left(\frac{\mathrm{Re}_{p\delta}}{8}\right)^{\frac{1}{n}} \qquad (3\text{-}28)$$

This expression contains two temporarily unknown constants $\mathrm{Re}_{p\delta}$ and κ. The velocity distribution is obtained as

$$\frac{v}{v_{max}} = \frac{1}{\kappa}\left[\sqrt{\frac{r}{R}} + \ln\left(1 - \sqrt{\frac{r}{R}}\right)\right] + \frac{1}{n\kappa}\ln\left[\mathrm{Re}_p\left(\frac{v_*}{c}\right)^{2-n}\right] - \frac{1}{\kappa}\left(1 + \frac{\ln \mathrm{Re}_{p\delta}}{n}\right) + \frac{6n+2}{n}\left(\frac{\mathrm{Re}_{p\delta}}{8}\right)^{\frac{1}{n}} \qquad (3\text{-}29)$$

The cross-sectional average velocity can be calculated in the usual way, and is found to be

$$\frac{c}{v_*} = \frac{v_{max}}{v_*} - \frac{1}{\kappa}\left(\frac{25}{12} - \frac{4}{5}\right) \qquad (3\text{-}30)$$

Thus

$$\frac{c}{v_*} = \frac{1}{n\kappa}\ln\left[\mathrm{Re}_p\left(\frac{v_*}{c}\right)^{2-n}\right] - \frac{1}{\kappa}\left(\frac{137}{60} + \frac{\ln \mathrm{Re}_{p\delta}}{n}\right) + \frac{6n+2}{n}\left(\frac{\mathrm{Re}_{p\delta}}{8}\right)^{\frac{1}{n}} \qquad (3\text{-}31)$$

The friction factor can be calculated in the same way for the Newtonian case:

$$\begin{aligned}\frac{1}{\sqrt{l}} &= \frac{0.8141}{nk}\lg\left(\mathrm{Re}_p\, l^{\left(1-\frac{n}{2}\right)}\right) + 0.7532\frac{n-2}{2n} \\ &+ 0.3535\left[\frac{6n+2}{n}\left(\frac{\mathrm{Re}_{pd}}{8}\right)^{\frac{1}{n}}\right] - \frac{1}{k}\left(2.283 + \frac{\ln \mathrm{Re}_{pd}}{n}\right)\end{aligned} \qquad (3\text{-}32)$$

Laboratory and in situ measurements by Navratil (1978) both provided similar value of $\mathrm{Re}_{p\delta} = 12.087$,

$$? = 0.407$$

These values are the same as those obtained for the Newtonian case. Thus, finally we can write

$$\frac{1}{\sqrt{\lambda}} = \frac{2}{n}\lg\left(\mathrm{Re}_p\,\lambda^{\left(1-\frac{n}{2}\right)}\right) + 1.511^{\frac{1}{n}}\left(\frac{0.707}{n} + 2.121\right) - \frac{4.015}{n} - 1.057 \qquad (3\text{-}33)$$

Or in a simple form

$$\frac{1}{\sqrt{l}} = 2\lg\left(3.715\frac{D}{k}\right) \qquad (3\text{-}34)$$

In the transition region between the friction factor curve for a smooth pipe and that for a wholly rough region, an interpolation formula can be obtained analogous to the Colebrook equation

$$\frac{1}{\sqrt{l}} = 2\lg\left[\frac{10^{\frac{-b}{2}}}{N_{\mathrm{Re}\,pp}^{\frac{1}{n}}\, l^{\frac{2-n}{2n}}} + \frac{k}{3.715D}\right] \qquad (3\text{-}35)$$

Szilas, Bobok, and Navratil (1981) further elaborated this equation. Friction factor charts based on the BNS equation are shown in Figure (3-4).and (3-5). The slope of friction factor curves for smooth pipe decrease as the behavior index decrease. The eventual laminar –turbulent transition is the other remarkable feature of the curves of the certain range of n. Experimental data obtained for crude oil pipelines with diameters ranging from 100mm to 600mm are in good agreement with the BNS equation. [28]

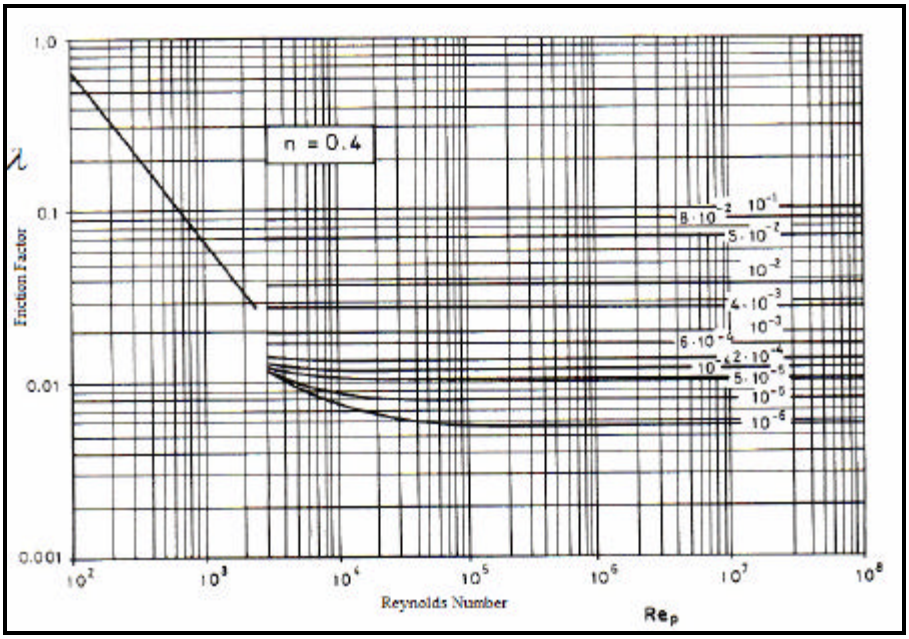

Fig. 3-4 Friction factor for turbulent flow of a pseudoplastic fluid n=0.4

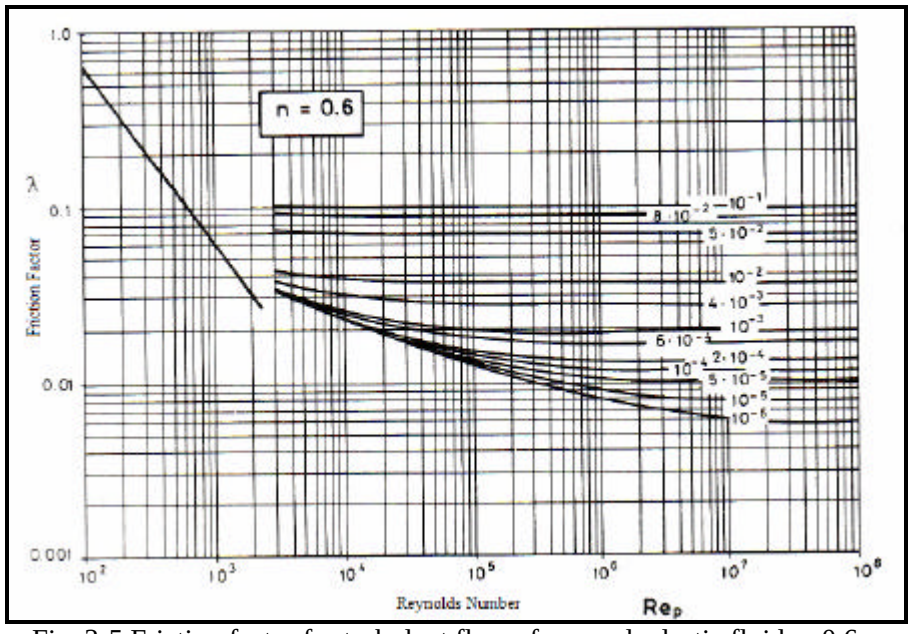

Fig. 3-5 Friction factor for turbulent flow of a pseudoplastic fluid n=0.6

3.4 Determination of Flow Curves

3.4.1 Introduction

The basic condition of determining a representative flow curves is to ensure that the flow behavior of the tested sample is the same as the fluid which will flow in the designed pipeline. The sampling, transport, storage and preparation of thixotropic-pseudoplastic crude samples must be made with special care. Three main difficulties must be considered:

1. The dispersed phase settles out in the dispersion medium.
2. Light hydrocarbon components are evaporating while storing.
3. Flow characteristics can be significantly influenced by the temperature and shear history.

3.4.2 Measurements with Extrusion Viscometer

The extrusion viscometer is the type of capillary or discharge viscometer where the fluid to be measured flows in the measuring section not because of gravity but due to the differential pressure occurring at the two ends of the measuring pipe section. [29]

3.4.3 Measurements with Rotary Viscometers

Several types of rotary viscometers are known, they are generally classified into two groups on the basis that they measure the torque and the angular velocity on the same, or different, structural element, respectively. These structural elements are generally coaxial cylinders but there are measuring elements of other shapes as well.

Rotary viscometers are more complicated then capillary ones. Their application is first advantageous for measurement of the flow behavior of Non-Newtonian fluids.

The main advantages are:

1. The shear stress belonging to adjusted shear rate can be determined at different shearing times.

2. The shear stress valid for steady state can be measured for different single shear rates.
3. The shear stress of the same sample can be determined at different shear rates, so it is suitable to determine the flow behavior of time dependent fluid.
4. The shear rate of the fluid sample in the viscometer only varies slightly, so it is possible to obtain the shear stress valid at the given shear rate.

Based on Dinsdale's theory we can discuss the scheme and measurement principles of a rotary viscometer. The principle scheme of the instrument is shown in Figure (3-6). Cylinder 2 is rotated with an adjustable angular velocity, w, and the developed torque is measured with the relative angular displacement of inside cylinder1. This cylinder is suspended on a torsional wire.

Let's suppose that the flow between the two cylinders is stationary, laminar, the end effect is negligible and no slippage occurs on the cylinder surface. [29]

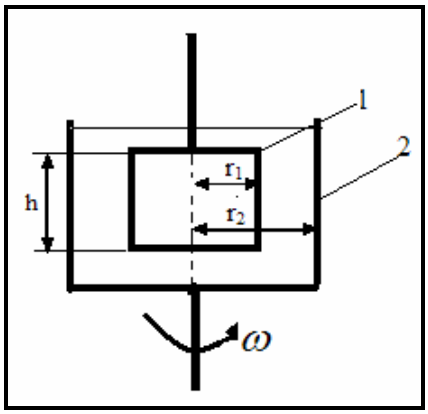

Fig. 3-6 Rotary viscometer.

The angular velocity in the fluid sample at a distance (r) from the shaft is, (w). Then the torque exercised by the outer fluid mantle upon the fluid cylinder of radius(r) is:

$$M = 2p.r^2 t_r \qquad (3\text{-}36)$$

$$t_r = \frac{M}{2p.r^2 h} \tag{3-37}$$

Where:

h :the height of the cylinder fluid.

t : shear stress.

r: the radius at each shear stress is generated.

The total differential of the equation $v = rw$ is

$$\frac{dv}{dr} = r\frac{dw}{dr} + w \tag{3-38}$$

The rate of shear depends only on the expression $r\frac{dw}{dr}$, is the velocity gradient in the case of pipeline flow, and it is different from the shear rate (*D*) For Newtonian fluid $t = m.D$ and thus by applying equations (3-32) and (3-33):

$$\frac{dw}{dr} = \frac{M}{2p.m.h.r^3} \tag{3-39}$$

If no slippage occurs on the pipe wall and at $r = r_1$, $w = 0$ and at $r = r_2$, the angular velocity w, of the rotating cylinder. These are the boundary conditions with which we can solve the equation, from which the torque:

$$M = \frac{4p.r_1^2 r_2^2.h.m.w}{r_2^2 - r_1^2} = cmw \tag{3-40}$$

Where:

c: is the instrument constant depending on the geometrical parameters of the instrument.

The average shear rate and average shear stress can be determined either as arithmetic or as a geometric mean. The mean shear stress is:

$$t = \frac{1}{2}(t_1 + t_2) = M\frac{r_1^2 + r_2^2}{4p.h.r_1^2 r_2^2.} \tag{3-41}$$

and $\bar{t} = m\overline{D}$ (3-42)

Where:

$\bar{t}$ is the average shear stress.

$\overline{D}$ is the average shear rate.

3.4.4 Haake Rot23 (100/300) Sensor System

To examine the crude oil transporting pipeline of Algyo, the pressure drop due to friction of crude oil flowing in the horizontal pipeline was calculated. To calculate the pressure drop the rheological properties of the crude were determined. To determine the rheological properties several laboratory measurements were made in the Petroleum Engineering Department of Miskolc University. Two kinds of oil were taken, one from Kiskunhalas and one from Algyo field, the two kinds of oil were tested and characterized by the help of Haake instrument, which is simply a rotary viscometer, connected to a Rheocontroller, with which we can adjust and control the variables needed for the measurement. These variables can be observed on a digital screen on the Rheocontroller.

3.4.5 Description

The system can give the basic required information about the fluids and with this we can classify and characterize them. The data from the Haake computer program enables us to determine some of the most important properties of the measured oil sample and generate a graph showing the behavior of the fluids under different conditions.

The system can measure:

- The shear stress.
- The shear rate.
- Their duration through the time.

- The viscosity.
- The pressure and its variation in time.
- Temperature

Fig. 3-7 Haake device.

Beside the sensor system of the rotary viscometer, Rotovisco RV 20, Rheocontroller RC 20, an additional heating circulating system and cooling system is necessary for the measurements. The sensor limits were as following: - maximum temperature 100°C, maximum pressure 300 bar, maximum shear stress 178 Pa, and maximum shear rate 500 1/s. Figure (3.7) describes the Haake instrument.[30]

3.5 Experimental Procedures

At the beginning of this chapter the theoretical background of flow curve measurements were introduced. In the following the steps of flow curve

measurements were taken with the results obtained being summarized. The samples were tested at different temperatures (5, 10, 20, 30, 40, 50, 60, and 70°C). The temperatures were selected considering the lowest soil temperature 5°C and the highest temperature that can be produced by the heating system.

3.5.1 Thixotropic Checking

The flow curve belonging to any shear duration of a thixotropic-psedoplastic oil looks like the flow curve of time-independent psedoplastic oil. The flow curve belonging to infinite shear duration is consequently suitable for determining the flow parameters of steady-state flow, and hence also the friction loss. In practice it is often found that after shear duration in the order of 10 minutes the flow curve approximates quite closely the values to be expected at infinite duration of shear. In designing relatively long pipelines for pressure drop, accuracy is little influenced by the fact that the pressure gradient is slightly higher in a short section near the input end than the steady-state value in the rest of the pipeline. When, however, relatively short pipelines are to be designed for pressure drop, the error due to use of the steady-state pressure gradient may be quite considerable.

Because the way of flow curve measurement differs if the oil has thixotropic behavior, for both oils, the shear stress at discrete shear speed was measured for a longer period of time. For each kind of fluid the thixotropic checking should be made, by testing both of the oils under soil temperature of 5°C and a slightly higher temperature of (20°C), during these measurements, the changing in shear stress vs. time is not too big.

This means that non of the oils have thixotropic behavior. The results are plotted in Figure (3-8), and (3-9).

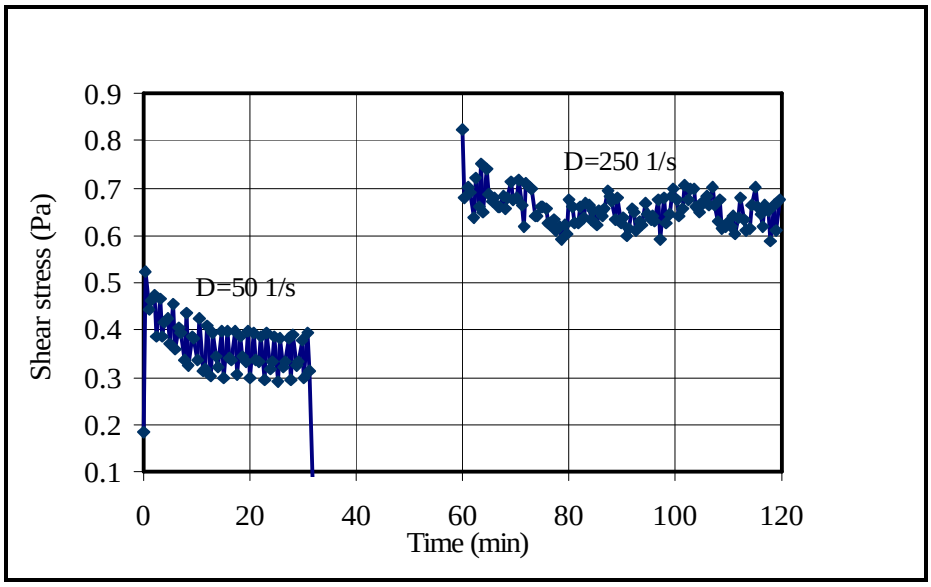

Fig. 3-8 Thixotropic checking for Algyo crude oil at 5ºC.

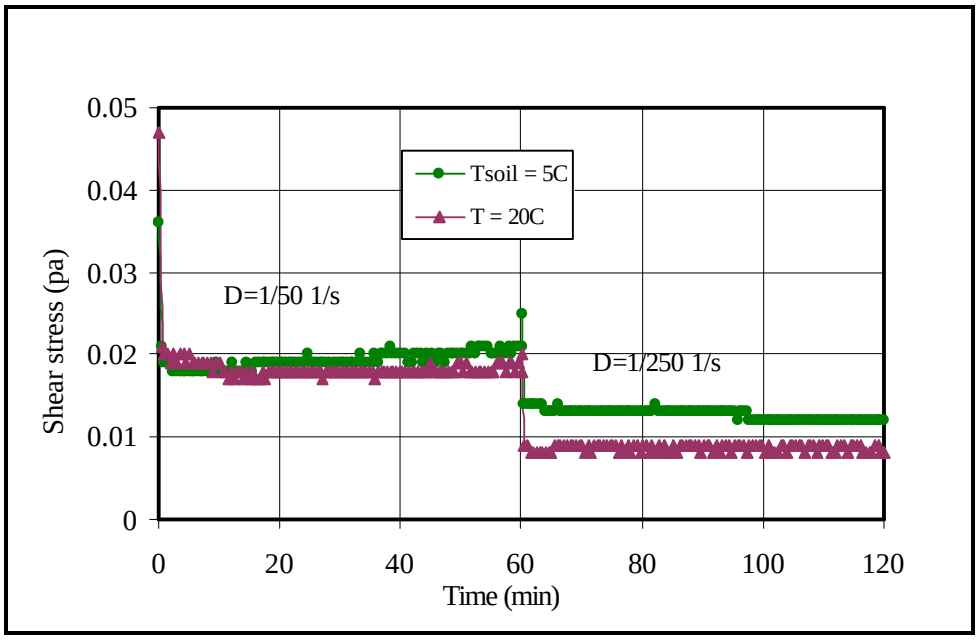

Fig. 3-9 Thixotropic checking for Kiskunhalas crude oil.

3.5.2 Flow Curves

From the results of thixotropic checking, it was clear that the flow curve measurement could be conducted by simple changing of the shear speed from zero to the measured value. The time at which the measured shear speed was reached varied in 20-30 minutes.

For examining the crude oil transporting pipeline of Algyo-Kiskunhalas – Szazhalombatta, calculating the pressure drop due to friction of crude oil flowing in the horizontal pipeline, and determining the rheological properties of the crude, some important variables have to be determined first.

3.5.3 The Laboratory Experiment

During the laboratory experiment the following steps were taken: -

1. Filling the stator with the crude oil sample, through the inlet port we can realize that the stator is completely filled with the crude oil after seeing the oil drops coming out from the out port in the stator.
2. The heating system, which is connected by rubber tube to the stator, is used to heat the crude oil until it reaches the required temperature. Refrigerating cooling system is also used here to control the temperature and keeping it at constant level.
3. Characterizing the sample by its name, under which measured temperature, and saving it as a data file.
4. To characterize the relationship between the shear stress (τ), and shear rate (D), we check the sample at a given temperature, from the zero to the maximum possible shear rate, D=5001/s.
5. From t/T , t/D relationships we chose t/D , to appear in the curve.

6. As result of plotted curve showing the relationship of τ/D, we can characterize the behavior of the crude oil sample under the specified temperature.
7. Crude oil samples have been checked under various temperatures with ranges from 5°C to 80°C.

3.6 Measurement Results

3.6.1 Algyo Crude Oil Sample

The Algyo crude oil sample has been tested at different temperatures. The flow curves of Algyo crude oil show the relation between shear speed and shear rate. As the shear speed increases the shear rate also increases but not at constant rate. So this means that the Algyo crude oil is a Non-Newtonian fluid. The curve-fitting program was used to fit a curve and to show the correlation coefficient, and from this coefficient we will know the behavior of this fluid.

3.6.2 Kiskunhalas Crude Oil Sample

Kiskunhalas crude oil sample was tested and checked under following temperatures: 70,50,40,20,10,5°C. To characterize the fluid we compare the relationship between shear speed and shear rate in each case at each of the aforementioned temperatures, by plotting a flow curve for each temperature. The slope of the curves appeared to be decreasing as the deformation rates increasing all the curves started from the origin of coordinates. From this way we can say that the crude oil of Kiskunhalas field is Non-Newtonian pseudoplastic or structural viscosity fluid, whose apparent viscosity is a function of shear stress.

The process of finding the best fit can be automated by letting Curve Expert to choose the best curve and determining the values of μ and n. Both the Algyo and

Kiskunhalas crude oil measurement and calculated results by curve fitting are shown in next tables and flow curve diagrams.

1. Algyo crude oil flow equation **:**

$$t = m' D^n \tag{3-43}$$

Table 3-1 Algyo crude oil rheological properties.

Temperature (°C)	*m`(Pa)*	***n***
5	0.116451	0.506433
20	0.181134	0.394185
30	0.074459	0.524587
40	0.228745	0.364927
50	0.125663	0.440634
60	0.169906	0.361184
80	0.179213	0.389109

2. Kiskunhalas crude oil properties

$$t = m' D^n \tag{3-44}$$

Table 3-2 Kiskunhalas crude oil rheological properties

Temperature (°C)	*m`(Pa)*	***n***
5	0.21992	0.57087
10	0.017277	0.89084
20	0.03111	0.75343
40	0.00121	1.22855
50	0.00422	1.03839
70	0.06901	0.57310

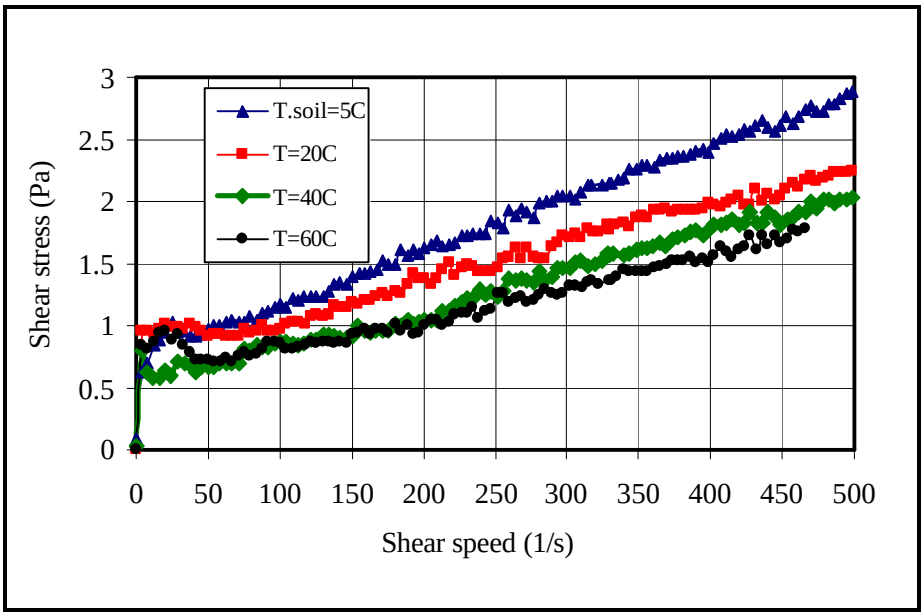

Fig. 3-10 Measured flow curves for Algyo crude oil.

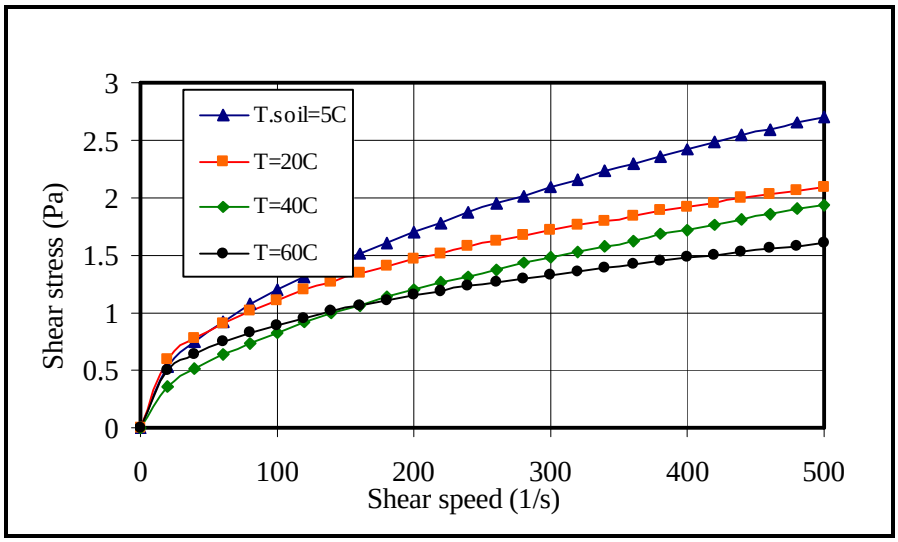

Fig. 3-11 Calculated flow curves for Algyo crude oil.

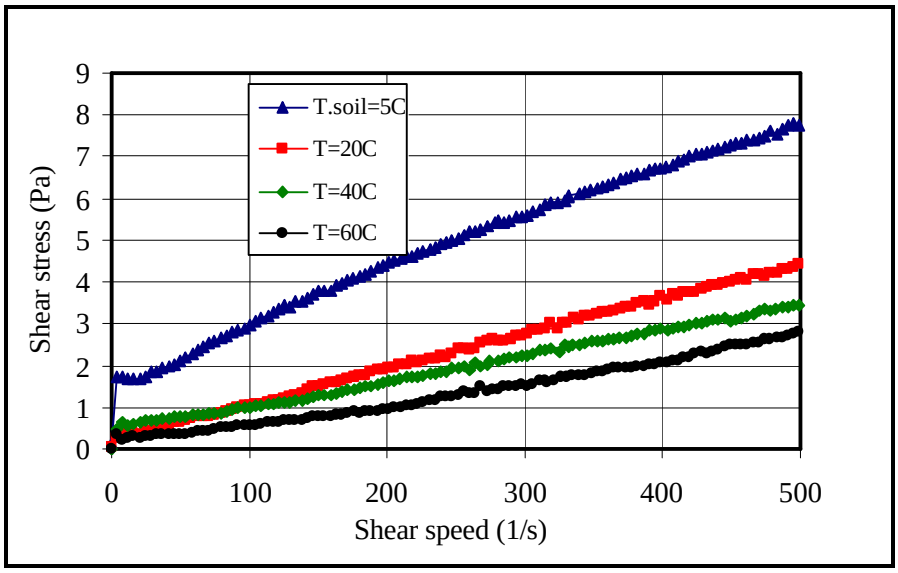

Fig. 3-12 Measured flow curves for Kiskunhalas crude oil.

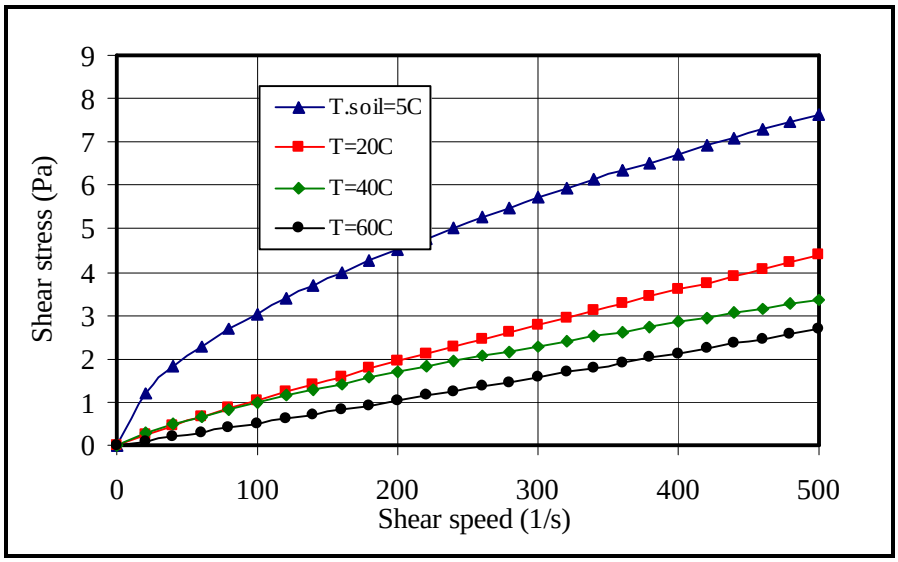

Fig. 3-13 Calculated flow curves for Kiskunhalas crude oil.

3.7 Density Measurement

The density of the two samples was measured at two different temperatures, to determine the density-temperature function of the oils The density-temperature functions were considered to be linear in the following form:-

$$r(T) = r_0 + a.T(above \cdot 0.0^0 C) \quad (3\text{-}45)$$

Where: -

ρ_O : Density at 0.0°C [kg/m^3]

α : Density correction factor [kg/m^3/°C]

T : Temperature above 0.0 °C.

The temperatures at which the measurements were taken were 20 and 50°C .The densities were determined measuring the mass and the volume of the crude at the temperatures mentioned.

Using the measured densities and temperatures the parameters of the equation (3.45) were determined.

The density-temperature equations for the two oils: -

- Algyo crude oil**:-**

$$r(T) = 817 - 1.007\,T(^oC) \quad (3.46)$$

- Kiskunhalas crude oil: -

$$r(T) = 804 - 0.7284\,T(^oC) \quad (3.47)$$

Table 3-3 Algyo and Kiskunhalas crude oil densities.

Temperature (°C)	Density (kg/m^3)	
	Algyo Crude Oil	**Kiskunhalas Oil**
5	812.465	801.158
10	807.43	797.516
20	797.36	790.232
40	777.22	775.664
60	757.03	761.096
70	747.01	753.812

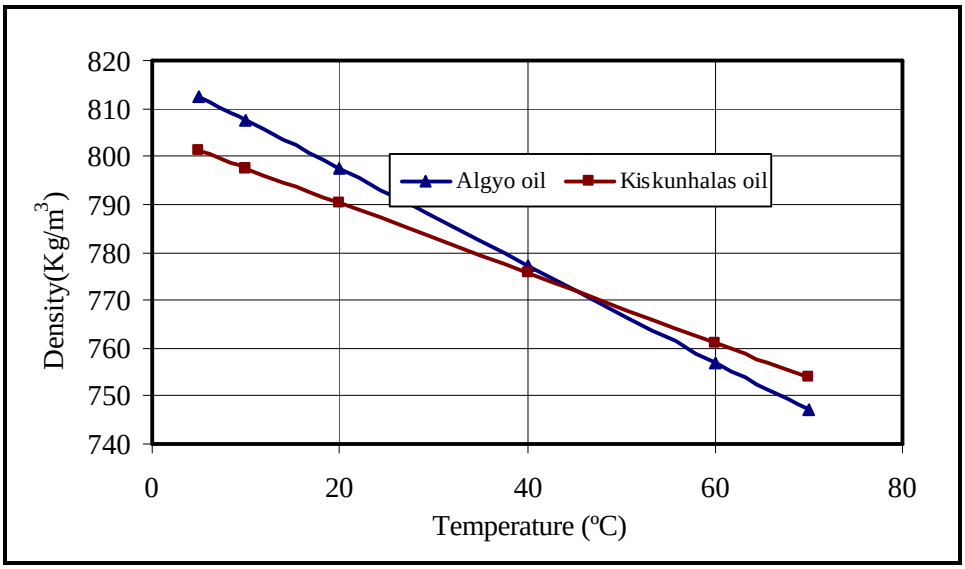

Fig. 3-14.Algyo and Kiskunhalas crude oil densities

CHAPTER 4
DEVELOPMENT OF A PROCEDURE TO DESCRIBE THE GROWTH OF PARAFFIN DEPOSITION IN PIPELINES

4.1 Introduction

Deposition of paraffins on the wall of crude oil pipelines is regarded as a problem since the pipe diameter is reduced. Therefore more power is required to force the same amount of crude oil through the system. In this part, a mathematical model is developed to calculate the paraffin formation and deposition in pipelines. The new method describes the growth of these deposits on the pipe wall. The description of the procedure is started with the theoretical explanation of the nature of these deposits followed by a discussion of non-isothermal pressure drop in pipeline. Temperature distribution along the pipelines and determination of friction factor for Non-Newtonian fluids are presented also.

4.2 Background Theories

Solid precipitation during production, transportation, and storage of petroleum fluids is a common problem faced by the oil industry throughout the world. Through complex phase transformations, dissolved and suspended solids (asphaltene, resins, paraffin and waxes) precipitate out of solution. Such phase segregations are sometimes followed by flocculation of the resulting precipitates. In many instance these depositions result in complete clogging of flow lines and serious damage to storage vessels and processing equipment (see Fig. 4-1). The solution or alleviation of the many technological problems posed by such deposition lies on a good

understanding of the interactions among the various parts in the local environment where phase segregation and flocculation takes place. [31]

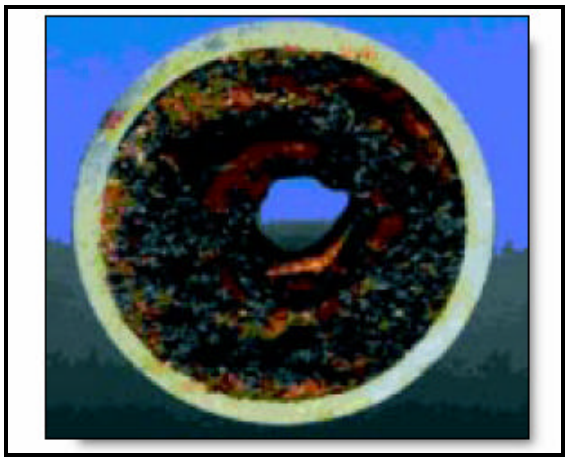

Fig. 4-1 Wax accumulation in crude oil pipeline.

Paraffin deposits, which form in well tubing and surface flowlines interfere with production and must be removed. Any organic deposit (heavy hydrocarbon deposit) associated with petroleum production is often called paraffin or wax. While paraffin compounds are usually the major component in these deposits, they are frequently a mixture of paraffins and asphaltenes. Their deposition in the formation, well conduits, flowlines and other production facilities leads to a decrease in production and an increase in operational problems.

No two crude oils are the same. Therefore, their paraffin and asphaltene compositions are different. Paraffin deposits, in addition to containing asphaltenes, may contain resins, gums, salt crystals, scales, clays, silts, sand and water. Paraffins are straight or branched chain nonpolar alkanes of relatively high molecular weight. Their chains usually consist of 20 to 60 carbon atoms with a melting range of 37-102°C. Asphaltenes, on the other hand, are high molecular weight cyclic aromatic compounds which usually contain nitrogen, oxygen and/or sulfur in their

molecular structure. Their melting range is higher than that of paraffins. Asphaltenes are usually negatively charged polar compounds.

In general, the lower the API gravity of the crude, the more asphaltenes are present, e.g., crude of 9 API gravity contains about 82% of asphaltene, whereas a crude of 41 API gravity contains only about 3% asphaltene. The presence of paraffin and asphaltene in the crude oil does not lead to problems in production or operation. It is their precipitation that leads to those problems. The precipitation and deposits of paraffins and asphaltenes are generally caused by a change in equilibrium conditions surrounding the produced petroleum, i.e., pressure, temperature, chemical composition, flow rates and/or electrostatic effects**.**

As the phenomenon of wax deposition in crude oil pipelines is of great relevance to the petroleum industry, there has been considerable work on both real and model oil pipeline systems in an effort to gain insight into the deposition process itself. It is generally believed that a thorough understanding of the mechanisms behind wax deposition will enable researchers to predict the growth and evolution of an incipient wax layer, allowing for the development of additives and surface treatments which will be more successful in hindering wax deposition. [32]

4.3 Calculations of Non-Isothermal Pressure Drop in the Pipelines.

4.3.1 Non-Isothermal Oil Transport

Most often pipelines transporting oil are buried in the ground. Therefore, if the oil viscosity is comparatively high and the temperature of the flowing oil differs appreciably from that of the pipeline’s environment the flow is considered to be non-isothermal and this is the case for the Algyo-Szazhalombatta pipeline studied.

4.3.2 Temperature distribution along the pipeline

If oil viscosity is high and the temperature of the flowing oil differs appreciably from that of the line's environment, flow can no longer be regarded as isothermal. Pipelines transporting oil are most often buried in the ground. The thermal behavior of the soil will accordingly affect the temperature of the flowing oil.

Assuming the heat flow pattern to be steady–state in and around the pipeline, the variation of axial oil temperature in the pipe can be determined. Part of the potential energy of the oil flowing in the pipeline is transformed into heat, will warm the oil. A relative increase in temperature will result also from the solid components separating out of the oil. The transfer of heat reduces oil temperature, from the pipeline into the lower-temperature environment. [33]

The temperature distribution along the pipeline can be calculated from the so-called Sukhov's equation. This equation assumes that the heat caused by friction losses and heat needed for solidification of parrafinic components is zero.

$$T_{f_2} = T_s + \left(T_{f_1} - T_s\right)\exp\left(\frac{kl}{qrc}\right) \tag{4-1}$$

Where: -

T_{f_1}: Oil temperature at the beginning of the pipe (in the centerline) (ºC)

T_{f_2}: Oil temperature at (l) distance from the beginning of the pipe. (ºC).

T_s: Soil temperature. (ºC)

k: Heat transfer coefficient. (W/mºC)

l: Distance from the beginning of the pipe. (m)

q: Flow rate.(m^3/s)

c: Specific heat of oil.(J/kg^{o}C)

ρ : Oil density. (kg/m3)

The heat transfer coefficient *k* shown in the next equation is an important parameter for calculating the temperature profile along a pipeline (Fig. 4-2). The following familiar equation shows the heat transfer coefficient *k* related to pipeline length for a buried, insulated pipeline section:

$$k = \frac{p}{\frac{1}{a_1 d_i} + \frac{1}{2 l_{in}} \ln \frac{d_{in}}{d_o} + \frac{1}{a_2 d_{in}}} \qquad (4\text{-}2)$$

Where:

k: Heat transfer coefficient (W/(m K))

d_i: Pipeline inside radius (m)

d_o: Pipeline out side radius (m)

d_{in}: Insulation outside radius (m)

α_1: Heat transfer coefficient inside pipeline (W/ (m^2K))

λ_{in} Heat conductivity of insulation (W/(m K))

α_2: Heat transfer coefficient outside pipeline insulation (W/ (m^2K))

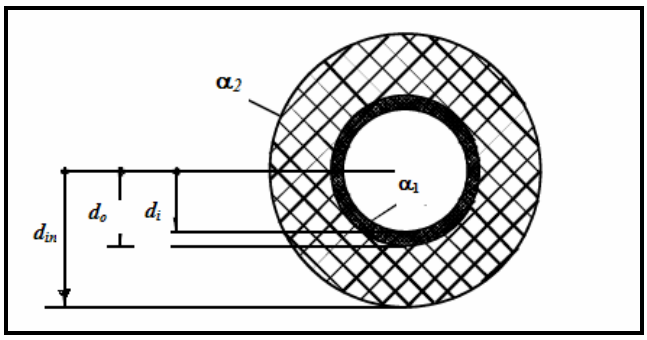

Fig. 4-2 Heat transfer coefficient related to pipeline diameter.

The third term in the denominator of equation (4-2) describes the thermal resistance of soil surrounding the pipeline. Assuming the original undisturbed temperature of the soil at pipeline depth to be T_s and the original-ground surface temperature to be equal to this value, it can be shown that:

$$a_2 = \frac{2l_s}{d_{in} \ln \frac{4h}{d_{in}}} \tag{4-3}$$

Where:

h: laying depth (m)

The approximation:

$a_2 = \frac{2l_s}{d_{in} \ln \frac{4h}{d_{in}}}$, will be the better, the greater is h/d_{in}. In most practical cases, that is, at about $h/d_{in} \geq 2$,the two formulae will furnish closely agreeing results; d_{in} denotes the OD of the pipeline as installed, together with insulation and coating.

Ford's procedure establishes the head loss of oil flowing in a pipeline by a finite-difference procedure. It permits us to account for the variation of heat transfer coefficient (*k*), and to use accurate friction-factor and viscosity values. Ford's theory

is started from the initial axial oil temperature (T_{f1}), by assuming an axial temperature drop (DT_f) of a few degrees(°C) to take place over a comparatively short, as yet unspecified length (L_1) of pipe. It is assumed that the average temperature over this length of pipe is, in a fair approximation,

$$Avg(T_{f1}) = T_{f2} - 0.5\Delta T_f \tag{4-4}$$

Using equations (4-1), (4-2) and (4-3), it is possible to calculate the length (L_1) over which the axial temperature drop is precisely (ΔT_f). In order to perform the calculation it is necessary to determine the heat transfer factor as indicated in equation (4-3) and, in the process, to find also the average wall temperature T_{i1}. Continuing the process, one obtains related values of T_f, T_i, T_{in} and l, which permits plotting the graph of temperature vs. length.

Viscosity values corresponding to the Reynolds number of N_{Re} = 2000, characterizing the transition from laminar to turbulent flow are calculated using the following equation:

$$N_{\mathrm{Re}} = \frac{v d_i}{n} \tag{4-5}$$

Where:

v: fluid velocity (m/s)

n : kinematic viscosity (m^2/s)

d_i: internal pipe diameter (m)

Also, oil temperature T_f corresponding to the critical velocity of the oil to be conveyed is read off the corresponding *T-v* graph. The point along the line where this temperature sets in will be where turbulent flow passes into laminar. In turbulent flow, as far as head loss calculations are concerned, pipeline cross-sectional

temperature may be equated to T_f. In laminar flow, however, the temperature differential between pipe axis and pipe wall is so significant that the average of the two, which will in fact determine the behavior of the crude has to be determined separately. [34]

4.3.3 Frictional pressure drop calculations

The total energy of the oil can be written in the following form at a distance of (x) from the input end of the pipeline:

$$P_1 + P_x + \left(\frac{v_1^{\,2} - v_x^{\,2}}{2} \right) r + (z_1 - z_x) rg = \Delta P_{fx} \qquad (4\text{-}6)$$

Where: -

P_1 : pressure at the input end .(Pa)

$P_{x:}$ pressure at (x) distance from the input end. (Pa)

v_1 : velocity at the input end.(m/s)

v_x : velocity at (x) distance from the input end.(m/s)

ρ : density of oil.(kg/m^3)

g : acceleration gravity.(m/s^2)

z_1: elevation at the input end of the pipe.(m)

z_x = elevation at (x) distance from the input end of the pipe.(m)

ΔP_{fx} = friction losses until the (x) point of the pipe.(Pa)

In equation (4-6) considering the oil to be incompressible, and the pipeline to have the same diameter, so that velocity does not change along the pipeline.

$$\left(\frac{v_1^{\,2} - v_x^{\,2}}{2} \right) r = 0$$

Then:

$$P_1 - P_x + (z_1 - z_x)rg = \Delta P_{fx} \tag{4-7}$$

Where: $(z_1 - z_x)rg$: hydrostatic pressure.

Pressure losses due to fiction of an incompressible fluid flowing in a horizontal pipe are given by the Darcy Weisbach equation:

$$\Delta P_f = l \frac{v^2 lr}{2d_i^{\,2}} \tag{4-8}$$

Friction factor for pseudoplastic fluids can be calculated as follows:

For laminar flow $$l = \frac{64}{N_{\mathrm{Re}\,pp}}$$

For turbulent flow:

$$\frac{1}{\sqrt{l}} = -2\lg\left[\frac{10^{\frac{-b}{2}}}{N_{\mathrm{Re}\,pp}^{\frac{1}{n}} l^{\frac{2-n}{2n}}} + \frac{k}{3.715 d_i}\right] \tag{4-9}$$

Where: $$N_{\mathrm{Re}\,pp} = \frac{d_i^{\,n} \bar{v}^{(2-n)} r}{\frac{K}{8}\left(6 + \frac{2}{n}\right)^n} \tag{4-10}$$

4.4 Description of the Growth of Paraffin Deposition in Pipelines

4.4.1 Introduction

This section contains the theoretical description of paraffin deposition growth in pipelines. All derivations are related to a small ? L section of the pipeline where paraffins from the transported oil deposit on the pipe inside wall. In order to describe the growth of the deposition thickness, the measured pressure drop occurring in the given pipe section needs to be known. Based on measurements made just after the last pigging operations, the relative roughness of the paraffin layer is calculated. It is easy

to see that this roughness is also valid at any other time, since the pipe inside wall can never be made completely clean and a small layer of paraffins is always present in the pipe.

Using a logic similar to the one given previously, the inside diameter of the pipe section at discrete times after the pigging operations needs to be calculated from pressure drop data. The task is accomplished using the calculation model developed in this dissertation, the detailed derivation of which is given in a subsequent section.

To describe the time variation of the paraffin layer thickness, and consequently the pipeline's inside diameter, a calculation model is developed which is based on measured pressure drops vs time. The last section of this part of the dissertation describes the proposed calculation of the additional pressure drop due to paraffin deposition.

4.4.2 Determination of Friction Factor and Pipe Roughness for a Clean Pipe

One basic problem of frictional pressure drop calculations is that the roughness of the pipe inside wall must be known. In our case the pipe inside wall is always covered by a paraffin layer and the steel material of the pipe is never exposed. This is due to the fact that pigging operations usually use a pig whose outside diameter is smaller than the pipe ID. It follows from the nature of pigging technology that the pipe can never be completely cleaned from paraffins and a clean pipe, as used in the following, only means that the paraffin thickness is reduced to such a level which is allowed by the pigging operations.

It can now be concluded that the actual roughness of any pipeline with paraffin inside layer never equals that of the original steel material. The actual roughness can be a function of the paraffin's behavior, the shape and surface conditions of the pig

used, etc. For our purposes it is sufficient to assume that the roughness of the paraffin layer is the same before and after pigging operations.

The determination of the relative roughness of the paraffin layer in oil pipelines is proposed as follows. If the frictional pressure drop in the given pipe section is known, then, based on the Darcy-Weisbach equation, the friction factor can be evaluated from which the ratio k/d is found from the BNS formula used for flow of non-Newtonian flow of pseudoplasic fluids. All calculations are done with pressure drop data measured at a time following a pigging operation thus ensuring that the conditions for a "clean pipe" are met.

The derivation of the proposed calculation model is started from the Darcy Weisbach equation:

$$\Delta P_f = l \frac{v^2 l r}{2 d_i^{\,2}} \tag{4-11}$$

Where:

ΔP_f = Pressure drop (Pa)

l = Friction factor

v =Velocity of fluid (m/s)

l = Pipeline length (m)

r = Fluid density (kg/m^3)

d_i = Internal pipe diameter (m)

In case of a clean pipe wall (original pipe diameter) the friction factor can be expressed from this equation as the following:

$$l = \frac{2 d_i \Delta P_f}{r v^2 l}$$

The pipe roughness can be determined from the BNS equation, used for Non-Newtonian fluids with pseudoplastic behavior

$$\frac{1}{\sqrt{l}} = -2\lg\left[\frac{10^{\frac{-b}{2}}}{N_{\mathrm{Re}\,pp}^{\frac{1}{n}} l^{\frac{2-n}{2n}}} + \frac{k}{3.715 d_i}\right]$$

Factors, b and n in the equation can be determined from the rheological indexes of flow curves presented in the third chapter

The BNS equation is arranged as follows:

$$10^{-\frac{1}{2\sqrt{l}}} = \left[\frac{10^{\frac{-b}{2}}}{N_{\mathrm{Re}\,pp}^{\frac{1}{n}} l^{\frac{2-n}{2n}}} + \frac{k}{3.715 d_i}\right]$$

The relative roughness of the pipe will be as expressed from the previous equation:

$$\frac{k}{D} = \left(10^{\frac{1}{-2\sqrt{l}}} - \frac{10^{\frac{-b}{2}}}{N_{\mathrm{Re}\,pp}^{\frac{1}{n}} l^{\frac{2-n}{2n}}}\right) 3.715 \qquad (4\text{-}12)$$

4.4.3 Development of the Mathematical Model to Describe the Influence of the Paraffin Deposition on the Pipe ID

The aim of the following mathematical solution is to determine the pipe internal diameter (affected by paraffin deposition on the pipe wall) for a given pipe section in case of the pressure drop occurring in the pipe section is known. During the process it is assumed, that the absolute roughness of the pipe does not change during the transporting, it is the same as determined for clean pipe (after pigging). The temperature of the pipe increment is considered to be constant as well.

The basis of the mathematical solution is the general friction drop equation:

$$\frac{\Delta p_f}{\Delta l} = l \frac{v^2 r}{2 d_i^{\,2}} \tag{4-13}$$

The left hand side of the equation (4-13) represents the friction gradient which is known from the measurement. The right hand side of the equation contains the internal pipe diameter (d_i). So, normally it is easy to express (d_i) from the equation. The main problem with this is that the velocity (v) and friction factor (l) are function of the internal pipe diameter (d_i) as well. To solve this problem we have to find an equation with which (v) and (l) are expressed as functions of (d_i). This equation is already introduced in the third chapter.

The average velocity of the flow can be expressed as the function of (d_i), using the following equation:

$$\bar{v} = \frac{4Q}{p\, d_i^{\,2}} \tag{4-14}$$

Where:

Q: flow rate in pipe section (m^3/s)

The friction factor (l), as described earlier, can be calculated using the well known BNS equation:

$$\frac{1}{\sqrt{l}} = -2\lg\left[\frac{10^{\frac{-b}{2}}}{N_{\mathrm{Re}\,pp}^{\frac{1}{n}}\, l^{\frac{2-n}{2n}}} + \frac{k}{3.715 d_i}\right] \tag{4-15}$$

As it is clear from equation (4-15), that (l) is a function of (d_i) and N_{Repp} as well, where N_{Repp} is described as:

$$N_{\mathrm{Re}\,pp} = \frac{d_i^{\,n}\, \bar{v}^{(2-n)} r}{\frac{K}{8}\left(6 + \frac{2}{n}\right)^n} \tag{4-16}$$

Here v and d are unknowns. To express N_{Repp} as a function of d_i only, let us introduce equation (4-14) into (4-16) then we get:

$$N_{\mathrm{Re}\,pp} = \frac{d_i^{\,n}\left(\dfrac{4Q}{p\,d_i^{\,2}}\right)^{(2-n)} r}{\dfrac{K}{8}\left(6+\dfrac{2}{n}\right)^{n}} \tag{4-17}$$

Because the temperature of the pipe increment is considered to be constant, some parameters of equation (4-17) will be constant as well. Let us collect them under a new name (a_1)

$$a_1 = \frac{r}{\dfrac{K}{8}(6+2/n)^{n}} \tag{4-18}$$

Rearranging equation (4-17) and introducing equation (4-18) in it we get:

$$N_{\mathrm{Re}\,pp} = d_i^{\,(3n-4)}\left(\frac{4Q}{p}\right)^{2-n} a_1 \tag{4-19}$$

After substituting $a_2 = \left(\dfrac{4Q}{p}\right)^{2-n}$ into equation (4-19) we get:

$$N_{\mathrm{Re}\,pp} = d_i^{\,(3n-4)} a_2 \tag{4-20}$$

To eliminate (l) from unknowns in eq. 4-15, let's express it from equation (4-13) as a function of (Δp) and substituting the equation (4-14) into it we can get:

$$l = \frac{\left(\dfrac{\Delta p}{\Delta l}\right) 2 d_i^{\,5}}{\left(\dfrac{4Q}{p}\right)^{2} r} \tag{4-21}$$

If we insert equations (4-20) and (4-21) into equation (4-15), the only unknown parameter will be the pipe internal diameter (d_i).and the equation will be in the following form:

$$\frac{1}{\sqrt{\frac{\left(\frac{?p}{?l}\right)2d_i^{\,5}}{\left(\frac{4Q}{p}\right)^2?}}} = -2\lg\left(\frac{10^{\frac{-ß}{2}}}{\left(d_i^{(3n-4)}a_2\right)^{\frac{1}{n}}\left(\frac{\frac{?p}{?l}2d_i^{\,5}}{\left(\frac{4Q}{p}\right)^2?}\right)^{\frac{2-n}{2n}}} + \frac{k}{3.71d_i}\right) \qquad (4\text{-}22)$$

To simplify equation (4-22), let's collect the parameters under new variable names as follows:

$$a_3 = \sqrt{\frac{2\left(\frac{?p}{?l}\right)}{\left(\frac{4Q}{p}\right)^2?}} \qquad (4\text{-}23)$$

$$a_4 = a_2^{\frac{1}{n}}\left(\frac{2\frac{?p}{?l}}{\left(\frac{4Q}{p}\right)^2?}\right)^{\frac{2-n}{2n}} = a_4 = a_2^{\frac{1}{n}}a_3^{2\left(\frac{2-n}{2n}\right)} \qquad (4\text{-}24)$$

Substituting (a_3) and (a_4) in equation (4-22) and rearranging it to get a more friendly form we get:

$$d_i^{\frac{5}{2}} = \frac{1}{-2a_3\lg\left(\frac{10^{\frac{-ß}{2}}}{d_i^{\frac{n+2}{2n}}a_4} + \frac{k}{3.71d_i}\right)} \qquad (4\text{-}25)$$

Checking equation (4-25), we can state it is a non-linear implicit function of pipe internal diameter (d_i). The solution of this equation gives the actual or affected pipe ID for a measured pressure gradient.

To solve such types of equations, at first I have tried the iteration method usually applied to get (l) from equation (4-15). Unfortunately, the solution did not

converge that is why I have tried a numerical method to arrive at the solution. In the following section a short description of the method used for numerical solution is presented.

4.4.3.1 Using the Numerical Solution

Newton's method is used to find an approximate solution of a univariate equation by simplified expands and factors expressions. Equations and systems of non-linear polynomial equations can easily be solved, yielding their real and complex solutions. Numeric operations are performed exactly, with no round-off error, and the results can be specified to thousands of digits of precision. By using Newton's method for solving the previously mentioned equation the pipe diameter and paraffin thickness in every section can be determined numerically.

4.4.4 Calculating the Pipe ID-Time Function

The pressure drop in the pipelines changes with time, as time increases, the pressure drop increases, too. This is due to a reduction of the internal pipe diameter as shown in Fig. 4-3. The figure schematically describes the influence of time on the pressure drop.

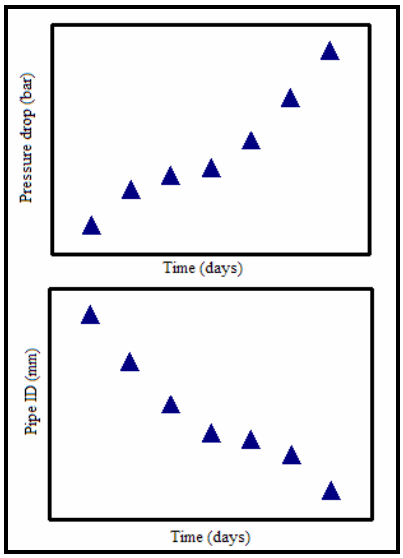

Fig. 4-3 Influence of time on the pressure drop and pipe ID.

Since the equation derived in the previous section determines the pipe diameter as influenced by paraffin deposition at a given time only, a procedure is applied here to find how the pipe diameter changes with time. By applying the previous equation for different times, (using measured pressure drops after the pigging operations), the variation of pipe diameter in time as shown in Fig. 4-3 can be determined.

To obtain intermediate estimates and to provide a simplified version of a complicated function, the discrete points on the pipe ID vs. time figure are to be curve fitted. In the following derivations, the functions best fitting the data for pressure drop and pipe diameter will be:

$$\Delta p = A \exp(b\,t) \tag{4-26}$$

Where:

Δp : pressure drop (bar)

A, b: constants

t: time (day)

$$ID = C \exp(d\,t) \tag{4-27}$$

Where:

ID: pipe (m)

C, d: constants

t: time (day)

CHAPTER 5
ECONOMIC CONDITIONS OF PIGGING OPERATIONS

5.1 Introduction

Pigging is a good way to manage wax deposition problems, with a few caveats:

- Pigging must be performed on a routine basis starting as soon as the temperature in the pipeline drops below the Wax Appearance Temperature (WAT).
- The pigging frequency must be sufficient to prevent excessive build up of wax between pigging runs.
- The right kind of pig must be used. In general, the pig must be able to provide sufficient force on the pipe wall to remove the deposit. A sphere is not capable of removing a wax deposit.

Although pigging can be an effective means of managing wax deposition, the actual cost of pigging needs to be thoroughly understood so that the economics of a project can be properly evaluated.

This chapter introduces the additional pressure drop calculations due to paraffin deposition on the pipe wall as well as the calculation of pumping cost due to additional pressure drop. In the last part, prediction of the most economic pigging interval for next pigging operations is presented

5.2 Pressure Drop Due to Paraffin Accumulation

Deposition of paraffin, as shown previously, entails an increased pressure drop in the pipeline. This continuously increases the power required to transport the oil

through the pipe. In the previous chapter, it was shown that the pressure drop increases with time and a correlation was also developed. Using the best-fitting equation found there, this section presents the calculation of additional pressure drop.

The pressure drop in case of a clean pipe wall (Δp_c) is calculated using the original diameter and is a constant value. But, the pressure drops for the influenced diameter (Δp_{in}) vary with time because the pipe ID varies with time as shown in the previous chapter. So, pipe diameters are calculated from equation (4-27) as a function of time and the pressure drops belonging to these diameters are also calculated. The time dependent additional pressure drop (Δp_{add}) can be determined as shown in the following equation:

$$\Delta P_{add}(t) = \Delta P_{in}(t) - \Delta P_c \tag{5-1}$$

Where:

$\Delta P_{add}(t)$: additional pressure drop due to paraffin deposition

$\Delta P_{in}(t)$: pressure drop in case of influenced pipe

ΔP_c: Pressure drop in case of clean pipe diameter.

Values of $\Delta P_{add}(t)$ are discrete values. Later, for iteration we need $\Delta P_{add}(t)$ as a real function of time. Curve fitting was used to get this function. We found that a function of the following form gives good results for fitting:

$$\Delta P_{add} = E \exp(f\ t) \tag{5-2}$$

Where:

E, f: parameters as the result from curve fitting

t: time (day).

5.3 Additional Pumping Cost

To calculate the hydraulic power required to move the oil through the pipeline, the following formula is used:

$$P_{hy} = \frac{Q\Delta P}{h} \tag{5-2}$$

Where

P_{hy}: the hydraulic power [W]

Q: pumping flow rate [m^3/s]

ΔP: pressure difference [N/m^2]

η : pump efficiency [%].

The additional pressure drop due to paraffin deposition was determined in the previous chapter where a best – fitting curve was found to have the following form:

$$\Delta P_{add} = E\ \exp(f\ t)$$

So, the hydraulic power will be

$$P_{hy} = \frac{Q}{?}\left(E\ \exp(f\ t)\right) \tag{5-3}$$

To calculate the work done due to paraffin deposition the following equation should be solved

$$dW = P_{hy}dt = \frac{Q}{?}\left(E\ \exp(f\ t\right)dt \tag{5-4}$$

The solution can be determined simply by integrating the equation:

$$W = \int P_{hy}dt = \frac{Q}{?}\int (E\ \exp(f\ t)\,dt$$

$$W = \frac{Q}{?}\left(\frac{E}{f}\ \exp(b\,t-1)\right) \tag{5-5}$$

If equation (5-5) is multiplied by the specific electricity cost, the cost of additional pressure drop can be calculated. The equation for additional cost is:

$$C = \frac{W\ Ce}{3600000} \tag{5-6}$$

Where:

W: work needed from equation (5-5)

Ce: Electricity cost (HUF/KWh)

5.4 Calculation of the most Economic Pigging interval

For the determination of the most economic interval we have to compare the cost of pigging operations with the additional cost due to additional pressure drop. This cost is expressed in the function of time by equation (5-6). The optimum time for the pigging is when the cost of pigging is equal to the additional transporting cost due to paraffin deposition. Substituting the cost of pigging into this equation the economic time interval can be expressed. A graphical solution was used to determine the economic interval. In a time-cost coordinate system the curve calculated from work equation is plotted as well as one pigging operation cost, it is a horizontal line in this coordinate system. The intersection of the two curves illustrates the most economic interval for the pigging operation as describes schematically in the Fig (5-1).

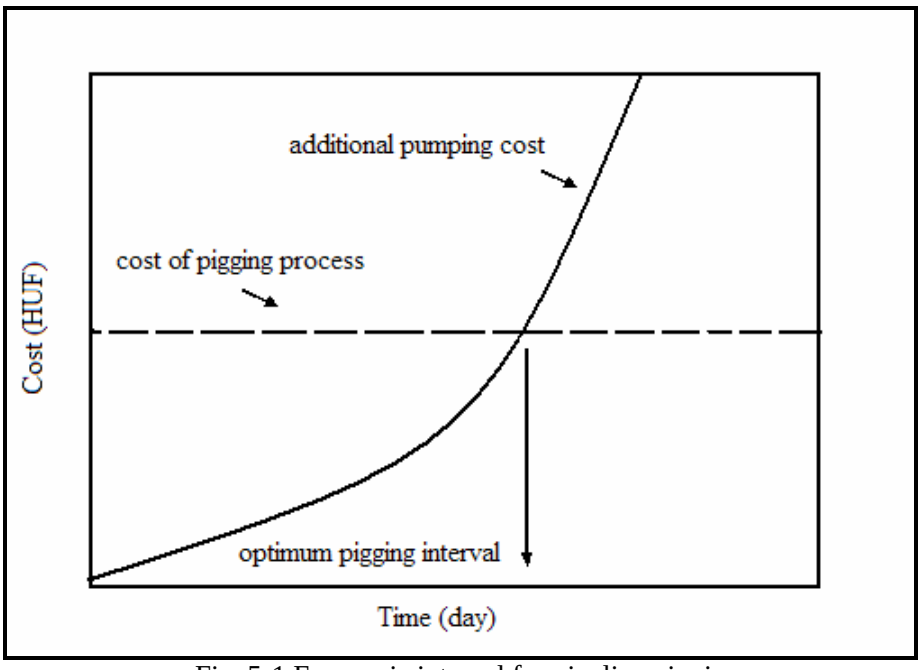

Fig. 5-1 Economic interval for pipeline pigging.

CHAPTER 6
CALCULATION RESULTS

6.1 Introduction

The main objective of this work is to determine the economic interval for the pigging in the Algyo-Szazhalombatta crude oil pipeline. Pipeline pigging is done not only for technical purposes but for economic ones, too. More importantly, the energy costs for pumping increase due to a reduced pipe diameter and an increased pipe wall friction. The option of the pipeline company is to regularly scrape and clean the wax from the pipeline walls.

To accomplish that, a procedure is applied here that focuses on the variation of pressure distribution due to pipe diameter changes which, in turn, are the result of accumulation of paraffin. A model was created by which the thickness of these deposits can be determined according to real field data obtained from the pipeline, and other variables such as temperature, pressure, and density. These data are rearranged and prepared for the calculations. Finally, the paraffin thickness vs. time function is derived. Overall, it becomes important to know the wax build-up rate at pipe walls in order to estimate treatment combinations and schedules. In fact, if a fairly accurate model can be obtained, operational parameters may be identified so as to prevent rather than cure the deposition problem.

6.2 Paraffins in the Algyo oil field

The Algyo field started to produce in 1965 and due to big orifice sizes used (6-10mm) and high flow rates 100-130 m^3/d, there were no problems concerning the

paraffin segregation. In 1967 experimental work done by using smaller orifice sizes led to thinking about the accumulation. Flow rate reductions by 60 m^3 were observed as a result of paraffin accumulations. Three crude oil samples were taken from three different wells in the Algyo field and tested for their properties by OGIL to find out the optimum method by which these deposits can be removed. The experimental results are shown in the following table and diagrams. [33]

Table 6-1.Paraffin Properties of Algyo oil

Crude oil properties	**Samples**		
	Sample no:1	**Sample no:2**	**Sample no:3**
Density at 20°C(gm/cm^3)	0.8072	0.8050	0.8621
Kinematic viscosity(cSt) 38°C 50°C 70°C	 3.7 2.38 1.78	 3.53 2.63 -	 14.5 9.4 5.67
Pour point (°C)	+18	+15	+24
Paraffin content (%)	8.21	7.43	6.45

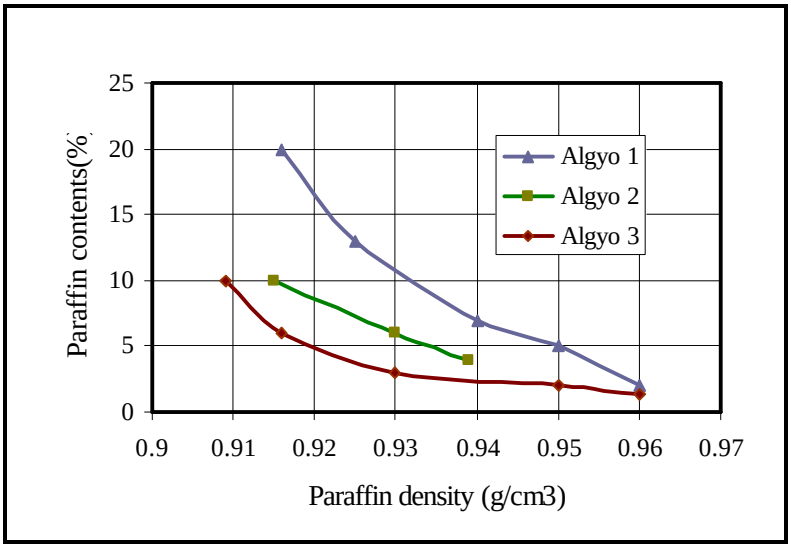

Fig. 6-1 Paraffin properties of Algyo crude oil samples at 20ºC.

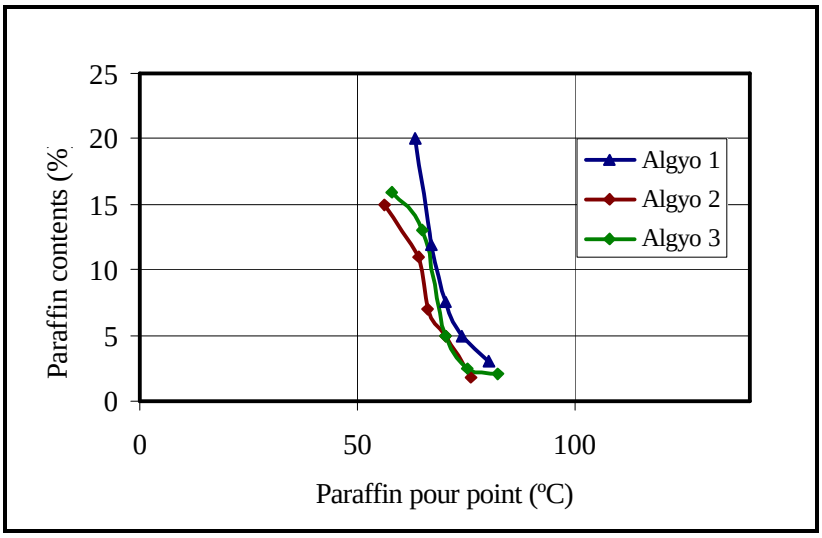

Fig. 6-2 Paraffin in Algyo field.

6.3 Paraffin deposition in the Algyo –Szazhalombatta pipeline

6.3.1 Field Data

The pipeline data is collected from the pipeline control system which is called supervisory control and data acquisition (SCADA). SCADA systems are computerized hardware and software systems that perform a set of monitoring and control functions. The system can also provide batch tracking, leak detection, and flow information. The remote terminal units (RTU) which already existed in the SCADA system were installed at compressor and pump stations and other remote sites. They measure operating conditions and transmit data to a central computer. Programmable logic controllers act as RTUs, but can also perform local logging and control functions at the remote site.

A key element of the pipeline consists of the following components, see Fig.6-3 :

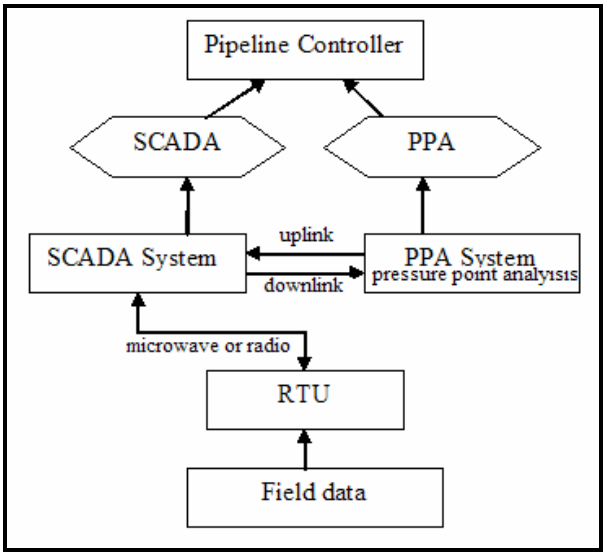

Fig. 6-3 Algyo-Szazhalombatta pipeline control system.

These data are collected carefully in a Microsoft Access file with a capacity of 600Mbyte indicating the variables for every second. In the following table one example is given.

Table 6-2 Sample of data collected from the pipeline

MQHTemp				
Time Stamp	**Value**	**Measured Quantity Token**	**Measure Quantity ID**	**Measured Parameter ID**
2004-01-15 00:00:14	0.7984	Algyo Fogyujto Sentinel számítómu FIYQ 101 méröág suruség	3505	6
2004-01-15 00:00:16	14.6215	Algyo Fogyujto Sentinel számítómu FIYQ 101 méröág hömérséklet	3507	3
2004-01-15 00:00:33	2.36	Kecskemét gerincnyomás Algyo vezeték PT3J001 (Algyo)	3127	1
2004-01-15 00:00:35	14.5784	Algyo Fogyujto Sentinel számítómu FIYQ 101 méröág hömérséklet	3507	3
2004-01-15 00:00:35	0.7969	Algyo Fogyujto Sentinel számítómu FIYQ 102 méröág suruség	3518	6
2004-01-15 00:00:55	17.5667	Algyo Fogyujto Sentinel számítómu FIYQ 102 méröág hömérséklet	3520	3
2004-01-15 00:01:16	0.7967	Algyo Fogyujto Sentinel számítómu FIYQ 102 méröág suruség	3518	6
2004-01-15 00:01:35	0.7985	Algyo Fogyujto Sentinel számítómu FIYQ 101 méröág suruség	3505	6
2004-01-15 00:01:35	14.5292	Algyo Fogyujto Sentinel számítómu FIYQ 101 méröág hömérséklet	3507	3
2004-01-15 00:01:35	0.7966	Algyo Fogyujto Sentinel számítómu FIYQ 102 méröág suruség	3518	6
2004-01-15 00:01:35	17.5157	Algyo Fogyujto Sentinel számítómu FIYQ 102 méröág hömérséklet	3520	3
2004-01-15 00:01:35	5.0128	Algyo gerincnyomás Algyo vezeték (Százhalombatta felé) PIT01	3550	1
2004-01-15 00:01:36	34.445	Algyo kilépo olaj homérséklet méro TT01	3557	3
2004-01-15 00:01:55	17.5037	Algyo Fogyujto Sentinel számítómu FIYQ 102 méröág hömérséklet	3520	3
2004-01-15 00:02:15	14.4857	Algyo Fogyujto Sentinel számítómu FIYQ 101 méröág hömérséklet	3507	3
2004-01-15 00:02:35	0.7965	Algyo Fogyujto Sentinel számítómu FIYQ 102 méröág suruség	3518	6
2004-01-15 00:02:35	17.4393	Algyo Fogyujto Sentinel számítómu FIYQ 102 méröág hömérséklet	3520	3
2004-01-15 00:02:35	34.39	Algyo kilépo olaj homérséklet méro TT01	3557	3

6.3.2 Use of Field Data

The data received is focusing only on five sections from the Algyo-Szazhalombatta pipeline. The raw data included two pigging cycles that were

converted into Excel files to facilitate the calculation procedure. This work focuses only on one pigging cycle and all calculations are based on the following table

Table 6-3 Data used for calculations.

Time (day)	**Temp (°C)**	**Density (kg/m^3)**	**Flow rate (m^3/d)**	**Pressures (bar)**				
				Algyo	***Soveny-haza***	***Palmono stora***	***Kiskunfel-egyhaza***	***Kecs-kemet***
21/01/2004	33.59	798.8		35.25	30.16	27.25	25.61	19.03
22/01/2004	32.88	797.4	142.5	35.28	31.98	28.88	27.64	21.82
24/01/2004	40.5	804.4	188.3	35.54	30.49	27.62	25.96	19.71
27/01/2004	33.49	792.5	183.6	34.72	29.67	26.88	25.3	19.11
29/01/2004	35.13	790.7	191.8	35.9	30.51	27.54	25.88	19.42
30/01/2004	34.45	792.8	192.2	35.11	29.67	26.6	24.96	18.74
31/01/2004	34.94	789.4	179.3	34.89	29.55	26.49	24.81	18.58
02/02/2004	37.48	790.3	189.2	35.76	30.35	27.21	25.51	18.93
03/02/2004	35.95	792.2	185.8	35.33	29.73	26.45	24.71	18.33
05/02/2004	38.19	791.2	181.4	35.35	29.98	26.78	25.02	18.37
06/02/2004	37.14	790.8	189.1	34.84	29.47	26.33	24.75	18.62
08/02/2004	37.32	792	188.7	35.13	29.59	26.16	24.48	18.21
09/02/2004	35.88	790.5	184.3	35.2	29.8	26.56	24.87	18.56
10/02/2004	37.37	789.2	172.3	36.28	30.51	27.15	25.34	19.01
11/02/2004	35.23	790.7	182.3	36.05	30.3	26.74	24.98	18.68
12/02/2004	35.28	791.3	193.3	35.88	29.86	26.51	24.75	18.41
14/02/2004	41.18	789.6	176	35.69	29.63	26.06	24.24	17.98
15/02/2004	38.84	790.4	174.5	35.57	29.82	26.37	24.65	18.23

6.4 Calculation Procedure

The following experimentally based table and graphs Fig. 6-4, 6-5 and Fig.6-6 illustrate the relation involving distance, height, and pressure before and after the pigging operations. The pressure is expressed in height to consider the effect of the geodetic height. The reduction of internal pipe diameter leads to greater pressure drop which leads to higher slope of the total energy curves. The difference between the two figures can be noticed, and it is due to paraffin precipitation on the pipe wall. The two

figures show that paraffin starts to deposit at a distance of 25 km (Sovenyhaza) till 90 km (Kecskemet). Otherwise in the first section there is no influence of paraffin due to temperature stability.

Table 6-4 The energy curves data.

Pipe section name	Distance (km)	Geodetic Height (m)	Before Pigging		After Pigging	
			Pressure (m)	Geodatic height+ Pressure (m)	Pressure (m)	Geodetic height+Pressure (m)
Algyo	0	80.4	365	445.4	340	420.4
Sovenyhaza	25.5	86.4	323	409.4	305	391.4
Palmonostora	42.5	92.6	275	367,6	256	348.6
Kiskunfelegyhaza	78.8	114.5	146	260.5	157	271.5
Kecskemet	99	140.2	111	251.2	122	262.2
Lajosmizse	113.2	128.4	103	231.4	103	231.4
Pusztavacs	137.6	97.4	92	189.4	90	187.4
Ocsa	153.9	100.8	64	164.8	74	174.8
Majoshaza	154.5	99.9	61	160.9	69	168.9
Szigetcsep	159.137	100.8	53	153.8	60	160.8
Szazhaombatta	161.36	143.6	43	186.6	51	194.6

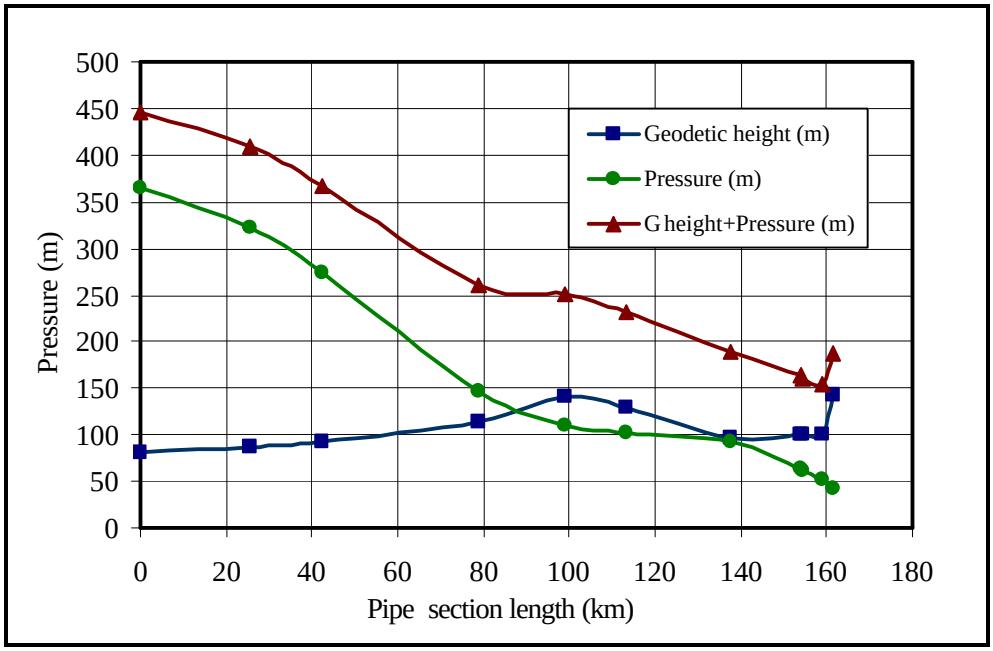

Fig. 6-4 Total energy curves before pigging.

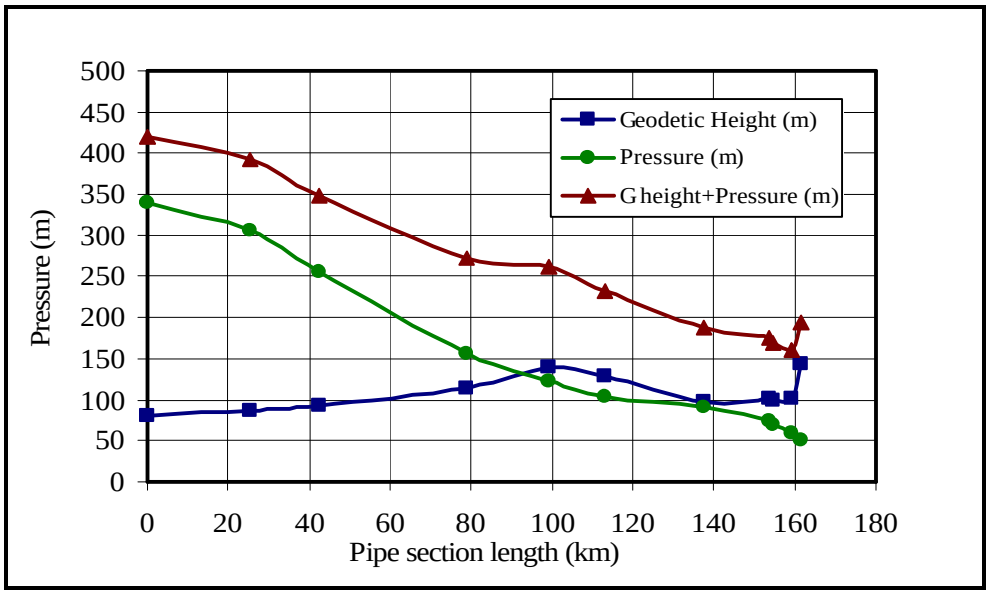

Fig. 6-5 Total energy curves after pigging

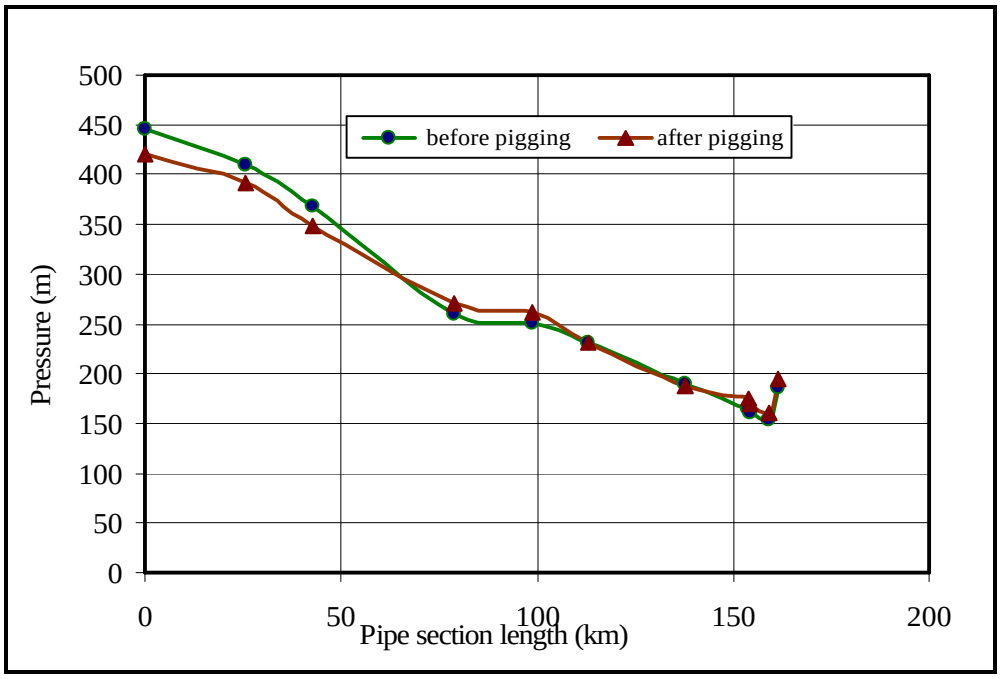

Fig. 6-6 Total energy curves before and after pigging.

To determine the thickness of the paraffin deposition, we use the total energy curves of the selected pipeline section. These curves are based on measured data. As it is well known, the pressure drop due to friction of an incompressible liquid flowing in a horizontal pipe is given by the Weisbach equation:

$$\Delta P_f = l \frac{v^2 l r}{2 d_i^{\,2}} \tag{6-1}$$

In case of a clean pipe wall the friction factor can be determined from this equation

$$l = \frac{2 d_i \Delta P_f}{r v^2 l} \tag{6-2}$$

According to the received data concerning the operation conditions of the Algyo –Szazhalombatta pipeline the calculations will focus on only 78 km length of the whole pipeline. This length is divided into three sections to get more accurate results and the friction factor for the three sections for a clean pipe (with an original diameter of 0.308 m) can be found in the following table.

Table 6-5 Friction factor for pipeline sections.

Section name	**Section length(m)**	**Friction factor (?)**
Sovenyhaza-Palmonostora	13377	0.027
Palmonostora-Kiskunfelegyhaza	10662	0.018
Kiskunfelegyhaza-Kecskemet	29254	0.024

6.4.1 Temperature distribution along the pipeline

The average temperatures in the pipeline sections were found by using Ford's Theory described previously. In the following table the section temperatures are shown as well as the rheological indexes for the average section temperature.

Table 6-6. Temperatures and rheological indexes.

Section name	Distance (km)	Temperature (°C)	Average Temperature (°C)	Rheological index
Sovenyhaza-Palmonostora	25.585 28.16 30.87 33.93 37.47	15 14 13 12 11	13	μ=0.113 n=0.506
Palmonostora-Kiskunfel-egyhaza	37.47 41.64 46.65 46.73 49.62	11 10 9. 9 8.6	10	μ=0.107 n=0.516
Kiskunfelegyhaza-Kecskemet	49.62 53.2 62.50 75.70 78.23 78.79	8.56 8 7 6.16 6.00 5.99	7	μ=0.0998 n=0.527

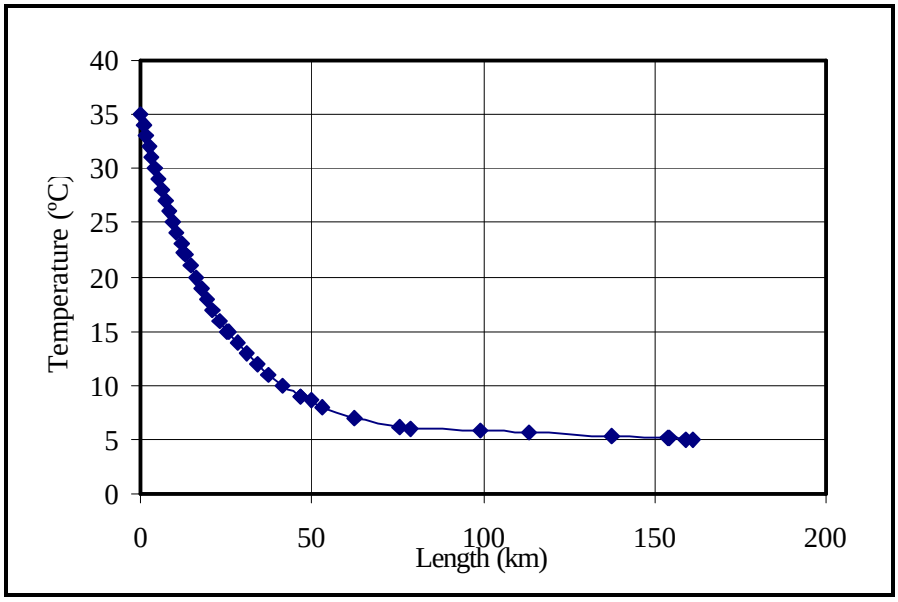

Fig. 6-7 Temperature distribution in Algyo-Szazhalombatta pipeline.

6.4.2 Determination of the pipe roughness from data taken from the clean pipe

In the following a method is developed to determine the influenced inside pipe diameter in every section separately. With reference to the current transportation schedule, around 180 m^3 of crude oil is transported from Algyo for 20 hours a day. During the remaining 4 hours 240 m^3 from both Algyo and Kiskunhalas as well. The two crude samples are mixed by 50% from each type of crude and the experiment shows that the flow properties of the mixed crude oil is not different significantly from the flow behavior of Algyo crude oil. Therefore, all calculations are made using the crude oil transported from Algyo only.

The pipeline was divided into three sections in order to get the performance parameters of the pipeline:

The input data for the calculations are the following:

- Pipeline length = 161.36 km
- Examined pipeline section 78 km
- External diameter = 324.8 mm
- Internal diameter =308 mm
- Heat conductivity of the insulation = 0.174 W/mk
- Maximum operating pressure = 64 bar
- Soil temperature =5, 10, 15 seasonal dependence

From equation (4-9), the relative roughness of the pipeline can be expressed as follow:

$$\frac{k}{D} = \left(10^{\frac{1}{-2\sqrt{l}}} - \frac{10^{\frac{-b}{2}}}{N_{\mathrm{Re}\,pp}^{\frac{1}{n}} \, l^{\frac{2-n}{2n}}} \right) 3.715 \qquad (6\text{-}3)$$

The factors n and b in the equation can be determined from the rheological indexes found in the previous chapter according to the section temperature. The friction factor (l), is determined from pressure drop equation in the case of clean pipe diameter and by knowing these values, the pipe section's roughnesses can be determined as shown in the following table

Table 6-7 Calculated pipeline roughness for all sections for clean pipe.

Section name	Section length(m)	Pipeline Roughness (m)
Sovenyhaza-Palmonostora	13377	0.0033
Palmonostora-Kiskunfelegyhaza	10662	0.00066
Kiskunfelegyhaza-Kecskemet	29254	0.00021

The Reynolds number can be determined by using the following equation:

$$N_{\mathrm{Re}} = \frac{d_i^{\,n}\,\bar{v}^{(2-n)'}\,r}{\frac{K}{8}\left(6+\frac{2}{n}\right)^n} \qquad (6\text{-}4)$$

Where:

n and K are constants and can be obtained from the measured flow curves.

The calculated Reynolds numbers are shown in the next table.

Table 6-8 Reynolds number for all sections.

Section name	Section length(m)	Temperature (°C)	Reynolds number
Sovenyhaza-Palmonostora	13377	13	6085.9
Palmonostora-Kiskunfelegyhaza	10662	10	6246.9
Kiskunfelegyhaza-Kecskemet	29254	7	6500

6.4.3 Determination of the Waxy ID of the Pipeline

As presented previously the pipe ID can be determined by using a suggested method which is in brief:

- Arranging the received field data

- The total energy curves which indicate the point at which paraffin starts to precipitate.
- Dividing the studied pipe length into three sections according to received measured data.
- Using the general pressure drop equations for the determination of friction factor in case of clean pipe as well as the roughness of the pipe from the BNS equation.
- Rearranging both the general pressure drop equation and the BNS for the determination of pipe diameter.

The following flow chart describes the suggested method

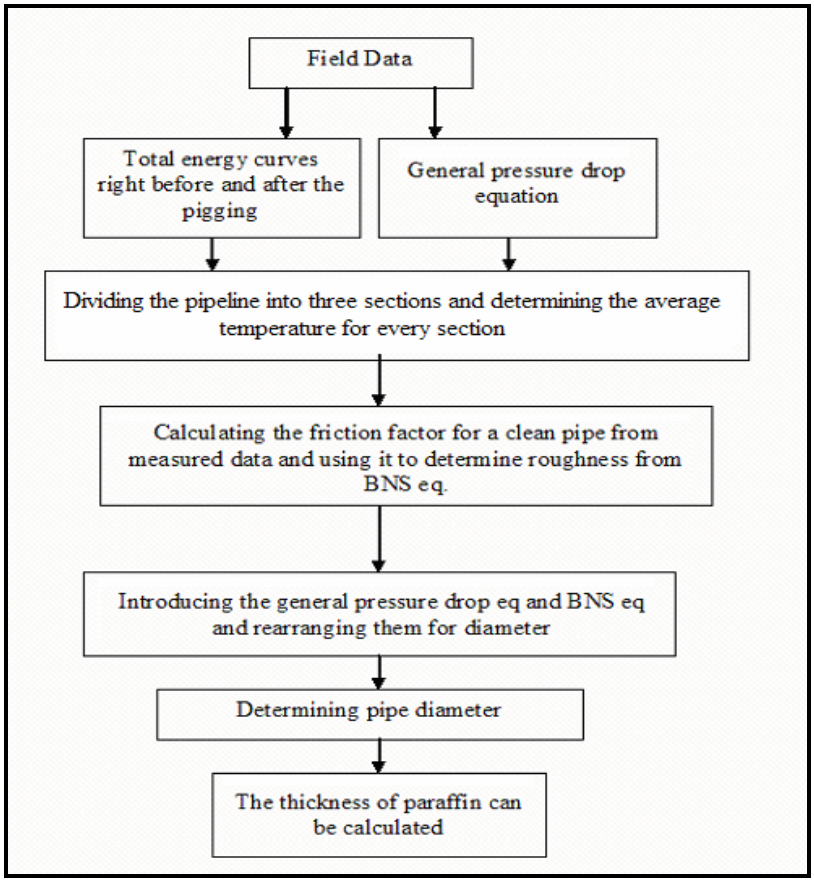

Fig. 6-8 Flow chart of the paraffin thickness calculation.

The derived equation for pipe ID calculation is in the following form:

$$d_i^{5/2} = \frac{1}{-2a_3 \lg\left(\frac{10^{-\beta/2}}{d_i^{n+2/2n} a_4} + \frac{k}{3.71 d_i}\right)} \quad (6\text{-}5)$$

In the following tables, the pipe diameter and paraffin thickness in the three sections with reference to section temperature (13ºC, 10ºC and 7ºC) are shown

Table 6-9. Sovenyhaza-Palmonostora section.

Time (day)	**a_1**	**a_2**	**a_3**	**a_4**	**Pipe diameter(m)**	**Paraffin thickness(m)**
1	17678.2	326.4	3.2	3035572	0.303	0.0025
2	17682.6	292.4	3.7	3588637	0.298	0.005
4	17813.3	310.9	3.4	3390301	0.296	0.006
7	17538.7	296.0	3.5	3346874	0.294	0.007
9	17509.9	315.2	3.5	3588552	0.292	0.008
10	17538.7	318.8	3.5	3680230	0.29	0.009
11	17470	294.8	3.7	3691001	0.288	0.01
13	17501	307.6	3.6	3837702	0.289	0.009
14	17543	299.9	3.8	4098060	0.285	0.011
16	17525	289.3	3.8	3949395	0.284	0.012
17	17512	307.4	3.6	3838917	0.284	0.012
19	17540	319.3	3.8	4895731	0.284	0.012
20	17505	295.8	3.8	4020180	0.285	0.011
21	17476.7	267.2	4.1	4238794	0.28	0.014
22	17563	291.9	4.0	4494043	0.288	0.01
23	17523	318.0	3.7	4225327	0.278	0.015
25	17534.3	290.2	4.0	4643223	0.276	0.016
26	17505.5	273.0	4.1	4373402	0.274	0.017

Table 6-10. Palmonostora-Kiskunfelegyhaza section

Time (day)	a_1	a_2	a_3	a_4	Pipe diameter(m)	Paraffin thickness(m)
1	18307.5	347.5	2.9	1775034	0.303	0.0025
2	18312.1	311.5	3.2	1882546	0.293	0.0075
4	18447.4	331.1	2.9	1751391	0.295	0.0065
7	18163	315.3	2.9	1574733	0.294	0.007
9	18133.2	335.6	3	1919665	0.294	0.007
10	18163	339.4	2.8	1707822	0.295	0.0065
11	18091.9	314	3	1704476	0.288	0.01
13	18124	327.5	3	1796419	0.285	0.011
14	18167.6	319.5	3.1	1859722	0.283	0.012
16	18149.7	308.2	3.1	1737181	0.279	0.014
17	18135.5	327.4	2.9	1617504	0.28	0.014
19	18165.3	339.9	2.7	1459325	0.28	0.014
20	18128.6	315	3	1781474	0.287	0.010
21	18098.8	284.8	3.4	1964478	0.285	0.0115
22	18188.2	311	3.1	1830111	0.29	0.009
23	18146.9	338.6	3	1889453	0.282	0.013
25	18158.4	309.2	3.2	1952103	0.281	0.0135
26	18128.6	290.9	3.3	1827108	0.277	0.016

Table 6-11. Kiskunfelegyhaza-Kecskemet section

Time (day)	a_1	a_2	a_3	a_4	Pipe diameter(m)	Paraffin thickness(m)
1	19226	375.5	3.4	2438373.7	0.303	0.0025
2	19230.8	336.9	3.7	2522750.3	0.298	0.005
4	19372.9	358	3.5	2307144.8	0.295	0.0065
7	19074.3	341	3.6	2279058.1	0.295	0.0065
9	19043	362.7	3.4	2333594.5	0.294	0.007
10	19074.3	366.8	3.4	2366470.2	0.294	0.007
11	18999.7	339.6	3.5	2233864.2	0.288	0.01
13	19033.4	354.1	3.6	2457394.9	0.289	0.0095
14	19079	345.4	3.6	2356435.3	0.285	0.012
16	19059.8	333.3	3.7	2537829.8	0.283	0.013
17	19045.4	353.9	3.4	2226390.9	0.283	0.013
19	19076.7	367.4	3.4	2309948.3	0.28	0.014
20	19038.2	340	3.6	2317878.4	0.279	0.014
21	19006.9	308.	3.8	2326240.4	0.277	0.015
22	19100.8	336.4	3.7	2378465.2	0.276	0.016
23	19057.5	365.9	3.4	2334479.7	0.276	0.016
25	19069.5	334.4	3.6	2248147.6	0.276	0.016
26	19038.2	314.8	3.8	2384911.5	0.272	0.018

The average effected pipe diameters and paraffin thicknesses in all sections are summarized in the following table and figures.

Table 6-12. Average effected pipe diameter and paraffin thickness.

Time (day)	Average pipe diameter(m)	Average pipe thickness(m)
1	303	0.0075
2	296	0.0175
4	295	0.019
7	294	0.0205
9	293	0.022
10	293	0.0225
11	288	0.03
13	287	0.0305
14	284	0.0355
16	282	0.039
17	282	0.0385
19	281	0.04
20	282	0.0365
21	282	0.041
22	278	0.038
23	277	0.044
25	275	0.0455

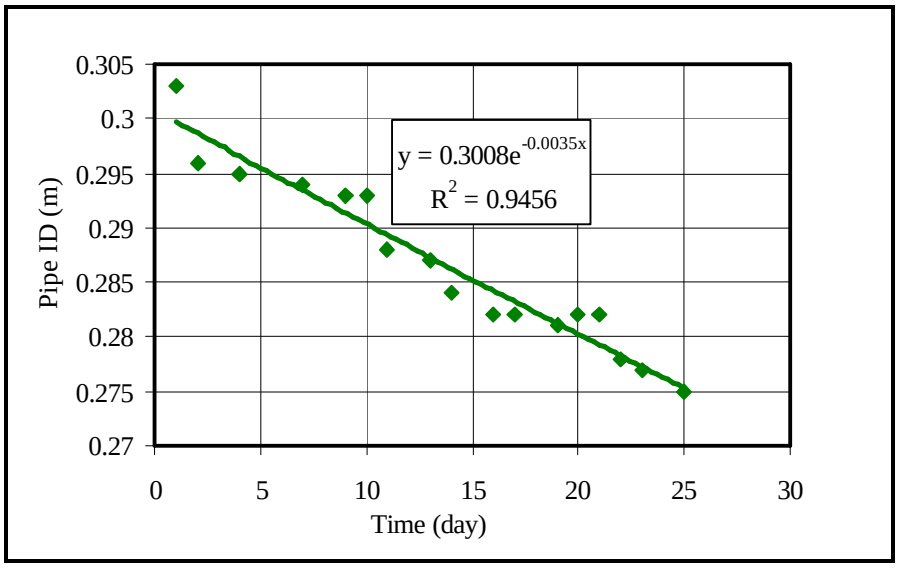

Fig. 6-9 Paraffin influence on pipe diameter.

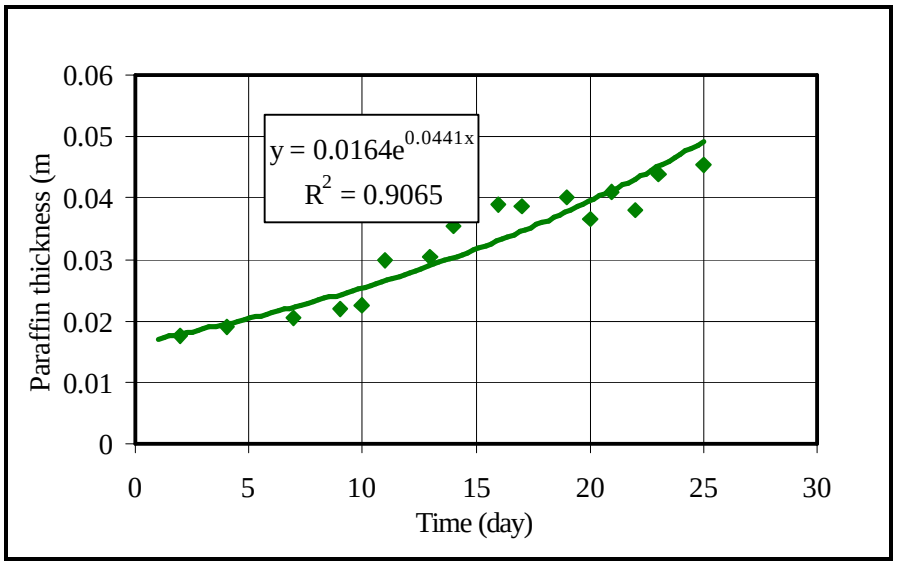

Fig. 6-10 Deposition thicknesses.

The final average equations concerning the thickness and pipeline diameter in the Sovenyhaza –Kecskemet section can be achieved by adding all sections

The equation for pipe diameter:

$$ID = 0.3\exp(-0.0035x) \tag{6-6}$$

The equation for paraffin thickness:

$$y = 0.016\exp(0.04x) \tag{6-7}$$

Where:

y: paraffin thickness (m)

x :time in days.

6.5 Determination of additional pressure loss vs. time equation

These calculations are based on calculated pipe diameters determined previously and the pressures in the sections belong to these diameters. as can be seen in the following table.

Table 6-13 Pressure at pipeline sections.

Time (day)	Pipe diameter (mm)	Pressure (bar)			
		Soveny-haza	Palmon-ostora	Kiskunfe-legyhaza	Kecs-kemet
1	303	32.43	30.04	27.45	20.03
2	296	35.82	33.16	30.23	22.08
4	295	36.34	33.64	30.66	22.4
7	294	36.88	34.14	31.67	22.73
9	293	37.43	34.64	31.55	23.06
10	293	37.43	34.64	31.55	23.06
11	288	40.36	37.92	33.96	24.84
13	287	40.98	37.92	34.47	25.22
14	284	42.95	39.72	36.08	26.41
16	282	44.33	40.99	37.21	27.24
17	282	44.33	40.99	37.21	27.24
19	281	45.01	41.65	37.8	30.49
20	282	44.33	40.99	37.21	27.24
21	282	44.33	40.99	37.21	27.24
22	278	47.28	43.71	39.64	29.03
23	277	48.06	44.43	40.28	29.51
25	275	49.68	45.92	41.61	30.49

The pressure drop resulting from the affected pipe diameter will be collected in the following table:

Table 6-14 Pressure drops between the sections

Pipe diameter (m)	Pressures (bar)		
	Sovenyhaza-Palmonostora	Palmonostora-Kiskunfelegyhaza	Kiskunfelegyhaza-Kecskemet
303	2.39	2.59	7.42
297	2.66	2.93	8.15
295	2.7	2.98	8.26
292	2.74	2.47	8.94
294	2.79	3.09	8.49
294	2.79	3.09	8.49
287	2.44	3.96	9.12
288	3.06	3.45	9.25
285	3.23	3.64	9.67
282	3.34	3.78	9.97
284	3.34	3.78	9.97
281	3.36	3.85	7.31
283	3.34	3.78	9.97
283	3.34	3.78	9.97
285	3.57	4.07	10.61
282	3.63	4.15	10.77
278	3.76	4.31	11.12

The total additional pressure drop for all given sections can be determined and an equation for pressure drop can be also determined.

Table 6-15 The total pressure drop.

Time (day)	Pipe diameter (mm)	Additional pressure drop (bar)
1	303	3.07
2	296	4.41
4	295	4.61
7	294	4.82
9	293	5.04
10	293	5.04
11	288	6.19
13	287	6.43
14	284	7.21
16	282	7.76
17	282	7.76
19	281	5.19
20	282	7.76
21	282	7.76
22	278	8.92
23	277	9.22
25	275	9.86

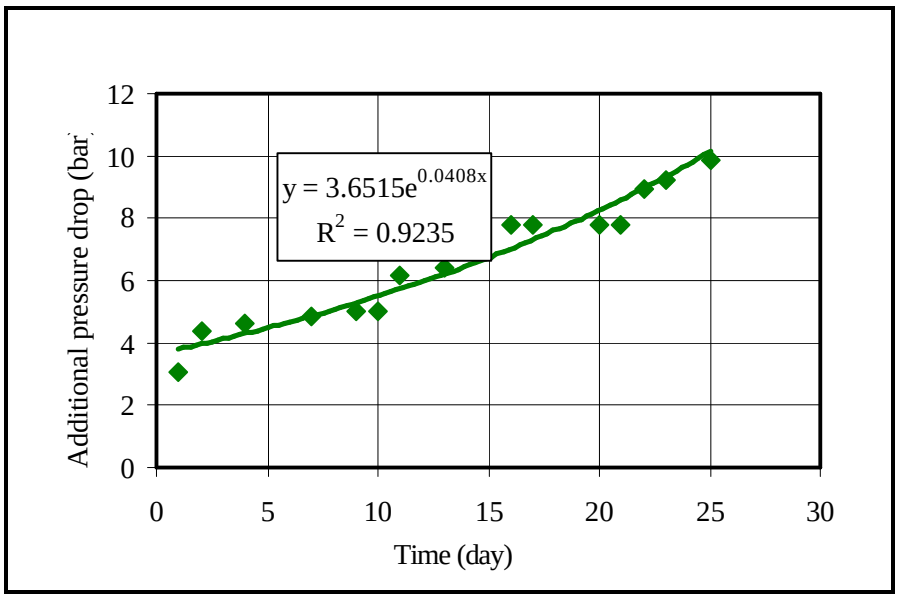

Fig.6-11 Additional pressure drop in Algyo-Szazhalombatta pipeline.

The determined equation is:

$$\Delta p = 3.6\exp(0.04t) \qquad (6\text{-}8)$$

6.6 Additional Pumping Cost due to Additional Pressure Drop

The derived work equation is shown in the following form:

$$W = \frac{Q.10^5}{?}\left(90\exp(0.04\,t - 1)\right) \qquad (6\text{-}9)$$

If the equation (6-9) is multiplied by the electricity cost, the cost of additional pressure drop can be calculated. The equation for additional cost is:

$$C = \frac{W.Ce}{3600000} \qquad (6\text{-}10)$$

Where:

Ce: Electricity cost (15HUF) for 1kW hour.

The additional pumping cost of three months can be determined by using the derived equation and the results are shown in the next table

Table 6-16 The additional pump cost.

Time (day)	Cost (HUF)
0	0
10	4426
20	11029
30	20881
40	35577
50	57501
60	90208
70	139001
80	211792
90	320384
100	482383
110	724057
120	1084593

6.7 Calculation of the most Economic Pigging interval

Pig cleaning is completed monthly to reduce the amount of paraffin wax build-up in the pipeline. This is the frequency MOL uses to clean the pipeline. A pig is manually sent into the pipeline at the pig launching station. The pig launching station is a designated area where the pipeline comes above ground so that a pig can be placed into the pipeline. The pig travels the length of the pipeline driven by the flow of the crude oil and the difference in pressure across the pig. The pig scrapes the paraffin wax from the pipeline walls and pushes the paraffin wax downstream.

To accomplish every project it is necessary to discuss its economic impact. In this study, the economic part is about the additional pumping costs due to additional pressure drop caused by paraffin deposition only. The total time between two pigging operations is 30 days, to calculate the pumping costs we have to consider the paraffin's ratio before pigging. The paraffin's thickness rate in every section was shown in the Fourth Chapter now we should calculate an average paraffin rate on all distances starting from 20 km till 86 km.

For the determination of the most economic interval into the work equation we have to substitute the cost of pigging process in order to solve it for time. A graphical solution was used to determine the economic interval. In a time-cost coordinate system the curve calculated from work equation is plotted as well as the pigging cost as a horizontal line. The intersection of the two curves illustrates the most economic interval for the pigging operation. The experimental table and graph are shown and the economic time interval for the pigging is about 62 days. This means that it is recommended to clean the pipeline every 62 days.

Table 6-17 The additional pumping cost and one pigging cost

Time (day)	Cost (HUF)	One pigging cycle(HUF)
0	0	108630
10	4426	108630
20	11029	108630
30	20881	108630
40	35577	108630
50	57501	108630
60	90208	108630
70	139001	108630
80	211792	108630
90	320384	108630
100	482383	108630
110	724058	108630
120	1084594	108630

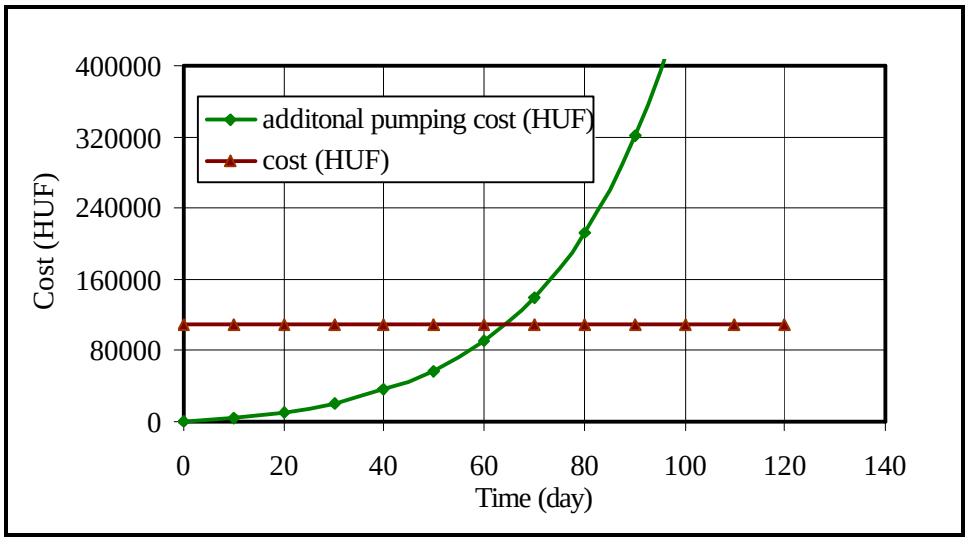

Fig. 6-12 Economic interval for Algyo-Szazhalombatta pipeline Pigging.

CHAPTER 7
CONCLUSIONS

Based on the results of my experimental and theoretical work I claim the following scientific findings:

1. My rheological measurements proved that none of the Algyo or the Kiskunhalas oils exhibit thixotropic behavior.
2. My measurements and their evaluation showed that the crudes transported in the pipeline investigated are Non-Newtonian and pseudoplastic fluids.
3. I clearly identified the influence of paraffin deposition on the operation of the pipeline from the analysis of the total energy curves calculated along the pipeline length. The influenced segment is situated between the 20 km and 78 km pipe sections.
4. I developed a calculation model for the determination of the pipeline's relative roughness at any pipe section. It is valid for the flow of pseudoplastic fluids and requires the measurement of the actual pressures along the pipeline only.
5. For the flow of pseudoplastic fluids in rough pipes I derived the appropriate formulas for the determination of the inside pipe diameter affected by paraffin deposition. The developed calculation model's input data are the measured flowing pressures vs. pipeline length. I fully

justified the assumption of a constant roughness for pipeline sections influenced by the paraffin deposition.

6. I developed a correlation, based on industry measurements, to describe the time change of the pipe inside diameter affected by the deposited paraffin layer.
7. Based on a simplified economic analysis I demonstrated how the crude transporting costs increase with time due to the increased amount of paraffin accumulated on the pipe inside wall. The economic model allowed the determination of the optimum pigging interval for the pipeline investigated.

LIST OF REFERENCES

1. Lozano, J.A. Fernandez Rodriguez, and Yidris, M, "A Study of the Rheological and conduct metric properties of two different Crude Oils and of their fractions using a modified Fan Viscosimeter" Society of Petroleum Engineers, SPE, 1976, p. 5979.

2. Matlach, W.J.and Newberry, M.E, "Paraffin Deposition and Rheological Evaluation of High Wax Content Altamont Crude Oils" Society of Petroleum Engineers, SPE, 1983, p. 11851.

3. Economides, M.J.and Chaney Jr., G.T, "The Rheological Properties of Prudhoe Bay Oil and the Effects of a Prolonged Flow Interruption on Its Flow Behavior" Society of Petroleum Engineers, SPE, 1983, p. 11711.

4. Yan, Dafan and Luo, Zheming: "Rheological Properties of Daqing Crude Oil and Their Application in Pipeline Transportation" Society of Petroleum Engineers, SPE, 1987, p. 14854.

5. Argillier, J.F. L. Barré, F. Brucy, J-L. Dournaux, I. Hénaut, R. and Bouchard, "Influence of Asphaltenes Content and Dilution on Heavy Oil Rheology" Society of Petroleum Engineers, SPE, 2001, p. 69711

6. Hénaut, L. Barré, J-F. Argillier, F. Brucy, R. and Bouchard, "Rheological and Structural Properties of Heavy Crude Oils in Relation With Their Asphaltenes Content "Society of Petroleum Engineers, SPE, 2001, p. 65020

7. Khan, S.A, Al-Marhoun, M.A, Duffuaa, S.O, Abu-Khamsin, and S.A, "Viscosity Correlations for Saudi Arabian Crude Oils" Society of Petroleum Engineers, SPE, 1987, p. 15720.

8. Wardhaugh, L.T, Boger, D.V and Tonner, S.P, "Rheology of Waxy Crude Oils" Society of Petroleum Engineers , SPE 1988, p. 17625

9. Argillier, J.F , C. Coustet, I and Hénaut, "Heavy Oil Rheology as a Function of Asphaltene and Resin Content and Temperature" Society of Petroleum Engineers, SPE, 2002, p. 79496

10. Sharma, Kuldip Saxena, V.K.Kumar, Avinish Ghildiyal, H.C.Anuradha, A. Sharma, N.D.Sharma, B.K and Dinesh, R.S, "Pipeline Transportation of Heavy Viscous Oil as Water Continuous Emulsion", Society of Petroleum Engineers, SPE,1998, p. 39537.

11. Ajienka, J.A and Ikoku, CU, "The Effect of Temperature on the Rheology of Waxy Crude Oils" Society of Petroleum Engineers, SPE, 1991, p. 23605.

12. Jessen, F.W. and Howell, J.N, "Effect of Flow Rate on Paraffin Accumulation in Plastic, Steel, and Coated Pipe, Trans". AIME (1958), issue, 213, p. 80-84.

13. Hunt, E.B, "paraffin deposition study using flow and cold-spot apparatuses" AIME, Petroleum Transactions, 1962, p. 1259-1269.

14. Bott, T.R. and Gudmundsson, J.S, "Deposition of Paraffin Wax from Kerosene in Cooled Heat Exchanger Tubes", Can. J. Chem. Eng., 1977, Vol. 55, p. 381.

15. Drayer and Dennis E, " Pipeline Transportation OFof Waxy, High Pour Point Crudes as Slurries" Society of Petroleum Engineers, SPE 1980, p. 9420

16. Burger, E.D; Perkins, T.K and Striegler, J.H, "Studies of Wax Deposition in the Trans Alaska Pipeline" Journal of Petroleum Technology, (1981), p. 1075-1068.

17. Weingarten, J.S.and Euchner, J.A, "Methods for Predicting Wax Precipitation and Deposition " Society of Petroleum Engineers, SPE, 1988, p. 15654

18. Majeed, A. Bringedal, B and Overa, S,"Model Calculates Wax Deposition for North Sea Oils" Oil and Gas Journal, 1990, p. 63-69.

19. Svendsen, J.A, "Mathematical Modeling of Wax Deposition in Oil Pipeline Systems" AIChE Journal 1993, 39 No. 8, p. 1377–1388

20. Brown, T.S. Niesen, V.G and Erickson, D, "Measurement and Prediction of the Kinetics of Paraffin Deposition" Society of Petroleum Engineers, SPE, 1993, p. 26548.

21. Hsu, J.J.C., Santamaria, M.M and Brubaker, J.P, "Wax Deposition of Waxy Live Crudes under Turbulent Flow Conditions" paper SPE, 28480 presented at the 1994 ATCE, New Orleans, p. 25-28 Sept.

22. Hamouda, A.A and Dividsen, S, "An Approach for Simulation of Paraffin Deposition in Pipelines as a function of Flow Characteristics with a Reference to Teesside Oil Pipeline" Society of Petroleum Engineers SPE, 1995, p. 28966.

23. Creek, J.L, Lund H.J, Brill J.P and Volk, M, "Wax deposition in single phase flow" Fluid Phase Equilibrium, 1999, Vo. 185, p. 801-811.

24. Singh, P. Venkatesan, R. Fogler, S.H. and Nagarajan, N, "Formation and Aging of Incipient Thin Film Wax-Oil Gels," AIChE J 2000,46 No.5, p. 1059-1074.

25. Nazar, A.R.S; Vaziri, H and Islam, M.R," Experimental and Mathematical Modeling of Wax Deposition and Propagation in Pipes Transporting Crude Oil" Society of Petroleum Engineers, SPE, 2001, p. 67328.

26. R. Shankar Subramanian, "Non-Newtonian Flows" www.clarkson.edu/project/ Subramanian/CH301/nots.

27. Rao, M.A. and Rizvi, S.S.H, "Engineering Properties of Foods", Marcel Dekker, New York, 1986

28. Bobok, Elemer, "Fluid Mechanics for Petroleum Engineers, Elsevier, 1993.

29. Szilas, A.P, "Production and Transport of Oil and Gas 1st part, Elsevier, 1975.

30. Haake Mess, "Instruction manual for rotary viscometer sensor system D100/300", 1989.

31. Dynora, Vasquez and Mansoori, G A, "Identification of Petroleum Precipitates", J. Petroleum Science and Engineering. Vol26, No 1-4, pp 49-56, 2000.

32. Elton, B and Hunt, J R, "Study of Paraffin Deposition", Pan American, PTE. Laboratory, 1962.

33. Szilas, A.P, "Production and Transport of Oil and Gas 2nd part, Elsevier, 1975.

34. Puskas, Sandor, "Paraffinkivalas az algyoi koolajtermelo kutatakban es vezetekeiben", Koolaj es Foldgaz. (120), No, 6, pp 171-175, 1987.

35. Ford, P.E "Pipeline for Viscous Fuels", Proceeding of 4th WPC, Section 8.